Gravitational Form Factor on the LF

$$A_f(q^2) = \int_0^1 x\, dx \int d^2\vec{\eta}_\perp e^{i\vec{\eta}_\perp\cdot\vec{q}_\perp} \tilde{\rho}_f(x, \vec{\eta}_\perp),$$

where

$$\tilde{\rho}_f(x, \vec{\eta}_\perp) = \int \frac{d^2\vec{q}_\perp}{(2\pi)^2} e^{-i\vec{\eta}_\perp\cdot\vec{q}_\perp} \rho_f(x, \vec{q}_\perp)$$

$$= \sum_n \prod_{j=1}^{n-1} \int dx_j\, d^2\vec{b}_{\perp j}\, \delta\Big(1 - x - \sum_{j=1}^{n-1} x_j\Big)$$

$$\times \delta^{(2)}\Big(\sum_{j=1}^{n-1} x_j \vec{b}_{\perp j} - \vec{\eta}_\perp\Big) \left|\tilde{\psi}_n(x_j, \vec{b}_{\perp j})\right|^2.$$

Extra factor of x relative to charge form factor

For each quark and

Integrate over angle

$$A_f(q^2) = 2\pi \int_0^1 dx\, (1-x) \int \zeta d\zeta\, J_0\left(\zeta q \sqrt{\frac{1-x}{x}}\right) \tilde{\rho}_f(x, \zeta)$$

$$\zeta = \sqrt{\frac{x}{1-x}} \left|\sum_{j=1}^{n-1} x_j \mathbf{b}_{\perp j}\right|$$

Gravitational Form Factor in AdS space

- Hadronic gravitational form-factor in AdS space

$$A_\pi(Q^2) = R^3 \int \frac{dz}{z^3} H(Q^2, z) \left|\Phi_\pi(z)\right|^2 ,$$

Abidin & Carlson

where $H(Q^2, z) = \frac{1}{2} Q^2 z^2 K_2(zQ)$

- Use integral representation for $H(Q^2, z)$

$$H(Q^2, z) = 2 \int_0^1 x\, dx\, J_0\left(zQ\sqrt{\frac{1-x}{x}}\right)$$

- Write the AdS gravitational form-factor as

$$A_\pi(Q^2) = 2R^3 \int_0^1 x\, dx \int \frac{dz}{z^3} J_0\left(zQ\sqrt{\frac{1-x}{x}}\right) \left|\Phi_\pi(z)\right|^2$$

- Compare with gravitational form-factor in light-front QCD for arbitrary Q

$$\left|\tilde{\psi}_{q\bar{q}/\pi}(x, \zeta)\right|^2 = \frac{R^3}{2\pi} x(1-x) \frac{\left|\Phi_\pi(\zeta)\right|^2}{\zeta^4},$$

Identical to LF Holography obtained from electromagnetic current

Holographic result for LFWF identical for electroweak and gravity couplings! Highly nontrivial consistency test

AdS/QCD can predict

- Momentum fractions for each quark flavor and the gluons $A_f(0) =< x_f >, \sum_f A_f(0) = A(0) = 1$
- Orbital Angular Momentum for each quark flavor and the gluons $B_f(0) =< L^3_f >, \sum_f B_f(0) = B(0) = 0$
- Vanishing Anomalous Gravitomagnetic Moment
- Shape and Asymptotic Behavior of $A_f(Q^2), B_f(Q^2)$

Note: Contributions to Mesons Form Factors at Large Q in AdS/QCD

- Write form factor in terms of an effective partonic transverse density in impact space $\mathbf{b}_\perp$

$$F_\pi(q^2) = \int_0^1 dx \int db^2 \, \widetilde{\rho}(x, b, Q),$$

with $\widetilde{\rho}(x, b, Q) = \pi J_0 \left[b \, Q(1-x)\right] |\widetilde{\psi}(x, b)|^2$ and $b = |\mathbf{b}_\perp|$.

- Contribution from $\rho(x, b, Q)$ is shifted towards small $|\mathbf{b}_\perp|$ and large $x \to 1$ as Q increases.

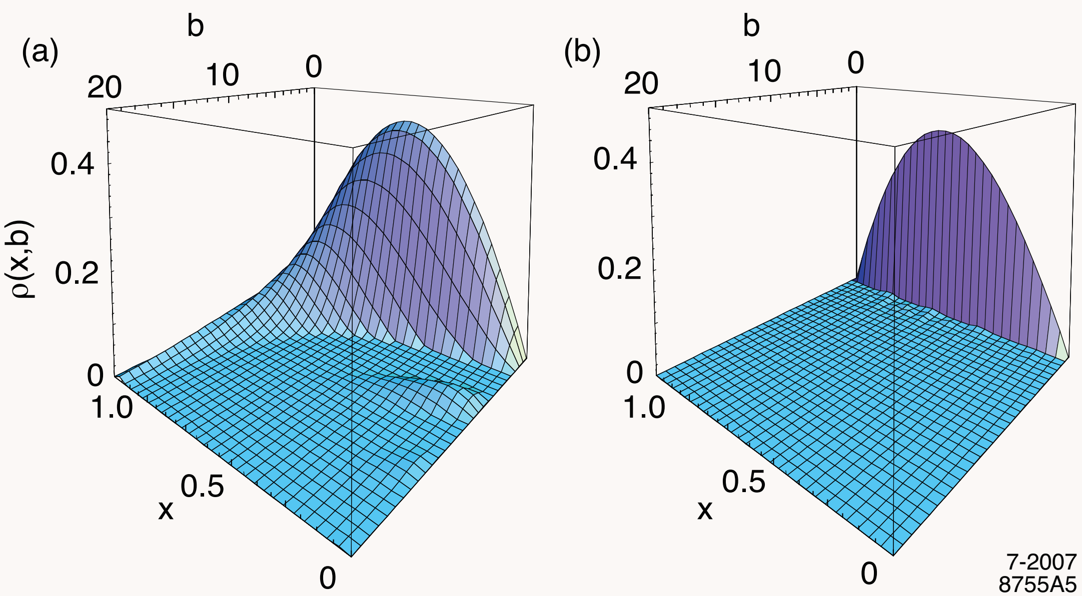

Fig: LF partonic density $\rho(x, b, Q)$: (a) Q = 1 GeV/c, (b) very large Q.

- Baryons Spectrum in "bottom-up" holographic QCD

GdT and Sjb hep-th/0409074, hep-th/0501022.

Baryons in Ads/CFT

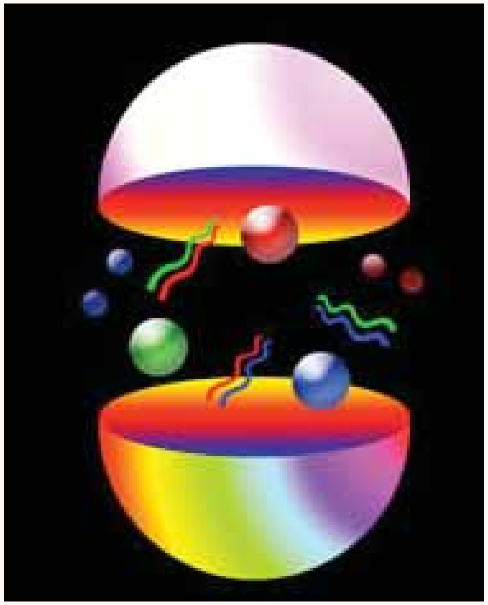

- Action for massive fermionic modes on AdS$_{d+1}$:

$$S[\overline{\Psi}, \Psi] = \int d^{d+1}x \sqrt{g}\, \overline{\Psi}(x,z) \left(i\Gamma^\ell D_\ell - \mu\right) \Psi(x,z).$$

- Equation of motion: $\left(i\Gamma^\ell D_\ell - \mu\right) \Psi(x,z) = 0$

$$\left[i \left(z\eta^{\ell m}\Gamma_\ell \partial_m + \frac{d}{2}\Gamma_z \right) + \mu R \right] \Psi(x^\ell) = 0.$$

Baryons

Holographic Light-Front Integrable Form and Spectrum

- In the conformal limit fermionic spin-$\frac{1}{2}$ modes $\psi(\zeta)$ and spin-$\frac{3}{2}$ modes $\psi_\mu(\zeta)$ are two-component spinor solutions of the Dirac light-front equation

$$\alpha\Pi(\zeta)\psi(\zeta) = \mathcal{M}\psi(\zeta),$$

where $H_{LF} = \alpha\Pi$ and the operator

$$\Pi_L(\zeta) = -i\left(\frac{d}{d\zeta} - \frac{L+\frac{1}{2}}{\zeta}\gamma_5\right),$$

and its adjoint $\Pi_L^\dagger(\zeta)$ satisfy the commutation relations

$$\left[\Pi_L(\zeta), \Pi_L^\dagger(\zeta)\right] = \frac{2L+1}{\zeta^2}\gamma_5.$$

- Note: in the Weyl representation ($i\alpha = \gamma_5 \beta$)

$$i\alpha = \begin{pmatrix} 0 & I \\ -I & 0 \end{pmatrix}, \qquad \beta = \begin{pmatrix} 0 & I \\ I & 0 \end{pmatrix}, \qquad \gamma_5 = \begin{pmatrix} I & 0 \\ 0 & -I \end{pmatrix}.$$

- Baryon: twist-dimension $3 + L \quad (\nu = L + 1)$

$$\mathcal{O}_{3+L} = \psi D_{\{\ell_1} \ldots D_{\ell_q} \psi D_{\ell_{q+1}} \ldots D_{\ell_m\}} \psi, \qquad L = \sum_{i=1}^{m} \ell_i.$$

- Solution to Dirac eigenvalue equation with UV matching boundary conditions

$$\psi(\zeta) = C\sqrt{\zeta}\left[J_{L+1}(\zeta\mathcal{M})u_+ + J_{L+2}(\zeta\mathcal{M})u_-\right].$$

Baryonic modes propagating in AdS space have two components: orbital L and $L + 1$.

- Hadronic mass spectrum determined from IR boundary conditions

$$\psi_\pm\left(\zeta = 1/\Lambda_{\rm QCD}\right) = 0,$$

given by

$$\mathcal{M}^+_{\nu,k} = \beta_{\nu,k}\Lambda_{\rm QCD}, \quad \mathcal{M}^-_{\nu,k} = \beta_{\nu+1,k}\Lambda_{\rm QCD},$$

with a scale independent mass ratio.

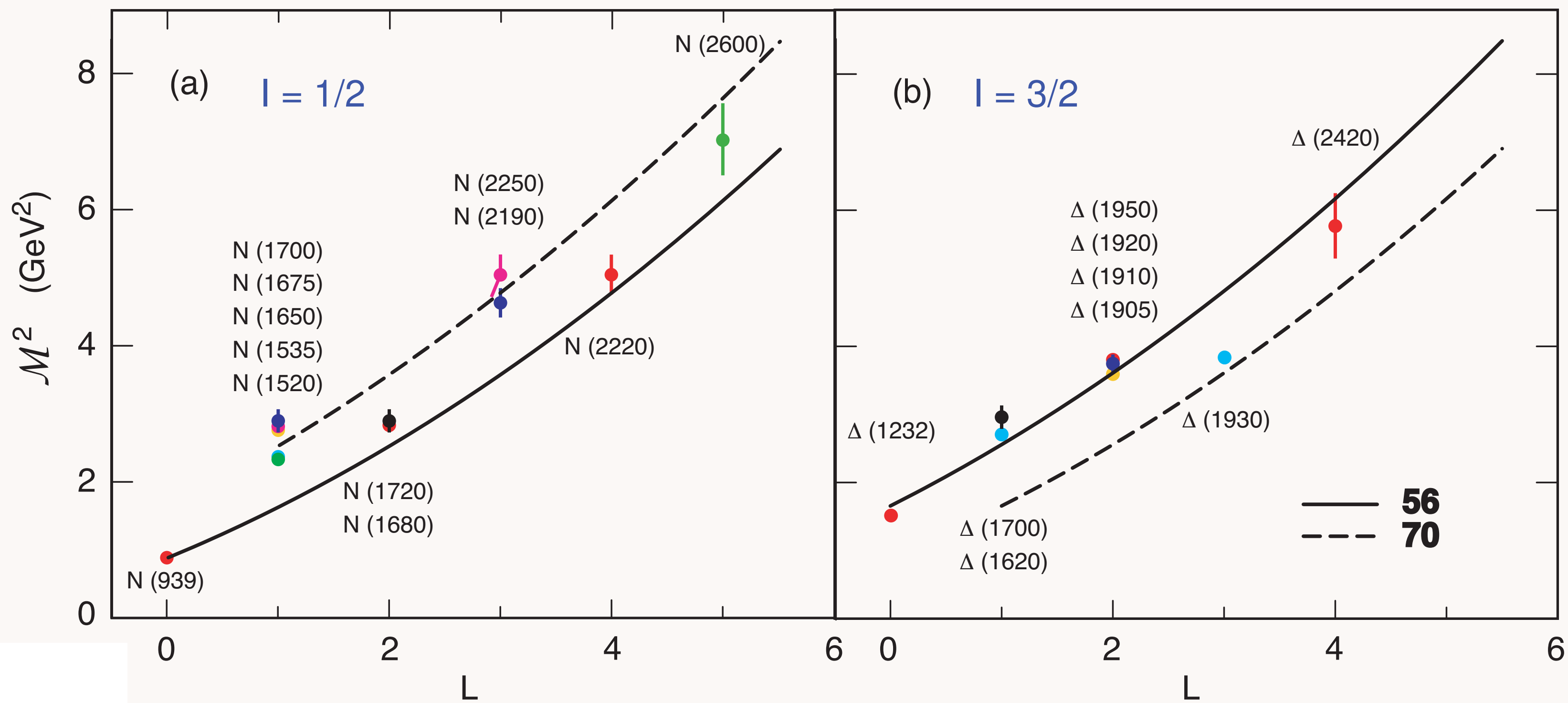

Fig: Light baryon orbital spectrum for Λ_{QCD} = 0.25 GeV in the HW model. The $\mathbf{56}$ trajectory corresponds to L even $P = +$ states, and the $\mathbf{70}$ to L odd $P = -$ states.

$SU(6)$	S	L	Baryon State
56	$\frac{1}{2}$	0	$N\frac{1}{2}^+(939)$
	$\frac{3}{2}$	0	$\Delta\frac{3}{2}^+(1232)$
70	$\frac{1}{2}$	1	$N\frac{1}{2}^-(1535)$ $N\frac{3}{2}^-(1520)$
	$\frac{3}{2}$	1	$N\frac{1}{2}^-(1650)$ $N\frac{3}{2}^-(1700)$ $N\frac{5}{2}^-(1675)$
	$\frac{1}{2}$	1	$\Delta\frac{1}{2}^-(1620)$ $\Delta\frac{3}{2}^-(1700)$
56	$\frac{1}{2}$	2	$N\frac{3}{2}^+(1720)$ $N\frac{5}{2}^+(1680)$
	$\frac{3}{2}$	2	$\Delta\frac{1}{2}^+(1910)$ $\Delta\frac{3}{2}^+(1920)$ $\Delta\frac{5}{2}^+(1905)$ $\Delta\frac{7}{2}^+(1950)$
70	$\frac{1}{2}$	3	$N\frac{5}{2}^-$ $N\frac{7}{2}^-$
	$\frac{3}{2}$	3	$N\frac{3}{2}^-$ $N\frac{5}{2}^-$ $N\frac{7}{2}^-(2190)$ $N\frac{9}{2}^-(2250)$
	$\frac{1}{2}$	3	$\Delta\frac{5}{2}^-(1930)$ $\Delta\frac{7}{2}^-$
56	$\frac{1}{2}$	4	$N\frac{7}{2}^+$ $N\frac{9}{2}^+(2220)$
	$\frac{3}{2}$	4	$\Delta\frac{5}{2}^+$ $\Delta\frac{7}{2}^+$ $\Delta\frac{9}{2}^+$ $\Delta\frac{11}{2}^+(2420)$
70	$\frac{1}{2}$	5	$N\frac{9}{2}^-$ $N\frac{11}{2}^-(2600)$
	$\frac{3}{2}$	5	$N\frac{7}{2}^-$ $N\frac{9}{2}^-$ $N\frac{11}{2}^-$ $N\frac{13}{2}^-$

Non-Conformal Extension of Algebraic Structure (Soft Wall Model)

- We write the Dirac equation

$$(\alpha\Pi(\zeta) - \mathcal{M})\, \psi(\zeta) = 0,$$

in terms of the matrix-valued operator Π

$$\Pi_\nu(\zeta) = -i\left(\frac{d}{d\zeta} - \frac{\nu + \frac{1}{2}}{\zeta}\gamma_5 - \kappa^2 \zeta \gamma_5\right),$$

and its adjoint $\Pi^\dagger$, with commutation relations

$$\left[\Pi_\nu(\zeta), \Pi_\nu^\dagger(\zeta)\right] = \left(\frac{2\nu + 1}{\zeta^2} - 2\kappa^2\right)\gamma_5.$$

- Solutions to the Dirac equation

$$\psi_+(\zeta) \sim z^{\frac{1}{2}+\nu} e^{-\kappa^2\zeta^2/2} L_n^\nu(\kappa^2\zeta^2),$$
$$\psi_-(\zeta) \sim z^{\frac{3}{2}+\nu} e^{-\kappa^2\zeta^2/2} L_n^{\nu+1}(\kappa^2\zeta^2).$$

- Eigenvalues

$$\mathcal{M}^2 = 4\kappa^2(n + \nu + 1).$$

- Baryon: twist-dimension $3 + L$ $\quad (\nu = L + 1)$

$$\mathcal{O}_{3+L} = \psi D_{\{\ell_1} \dots D_{\ell_q} \psi D_{\ell_{q+1}} \dots D_{\ell_m\}} \psi, \qquad L = \sum_{i=1}^{m} \ell_i .$$

- Define the zero point energy (identical as in the meson case) $\mathcal{M}^2 \rightarrow \mathcal{M}^2 - 4\kappa^2$:

$$\mathcal{M}^2 = 4\kappa^2 (n + L + 1).$$

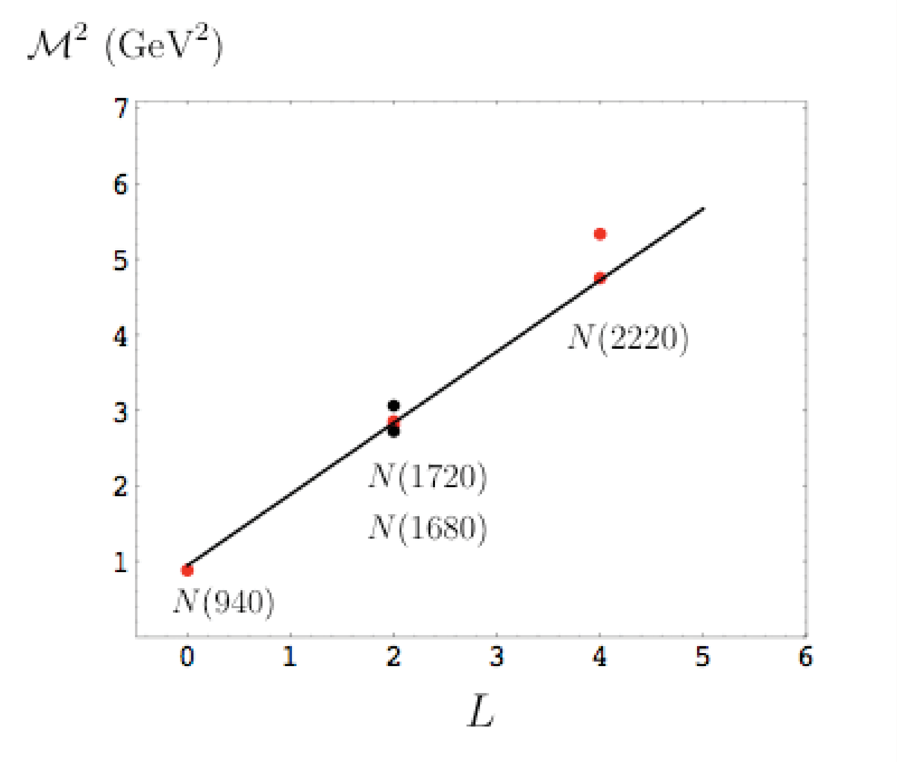

Proton Regge Trajectory $\quad \kappa = 0.49$GeV

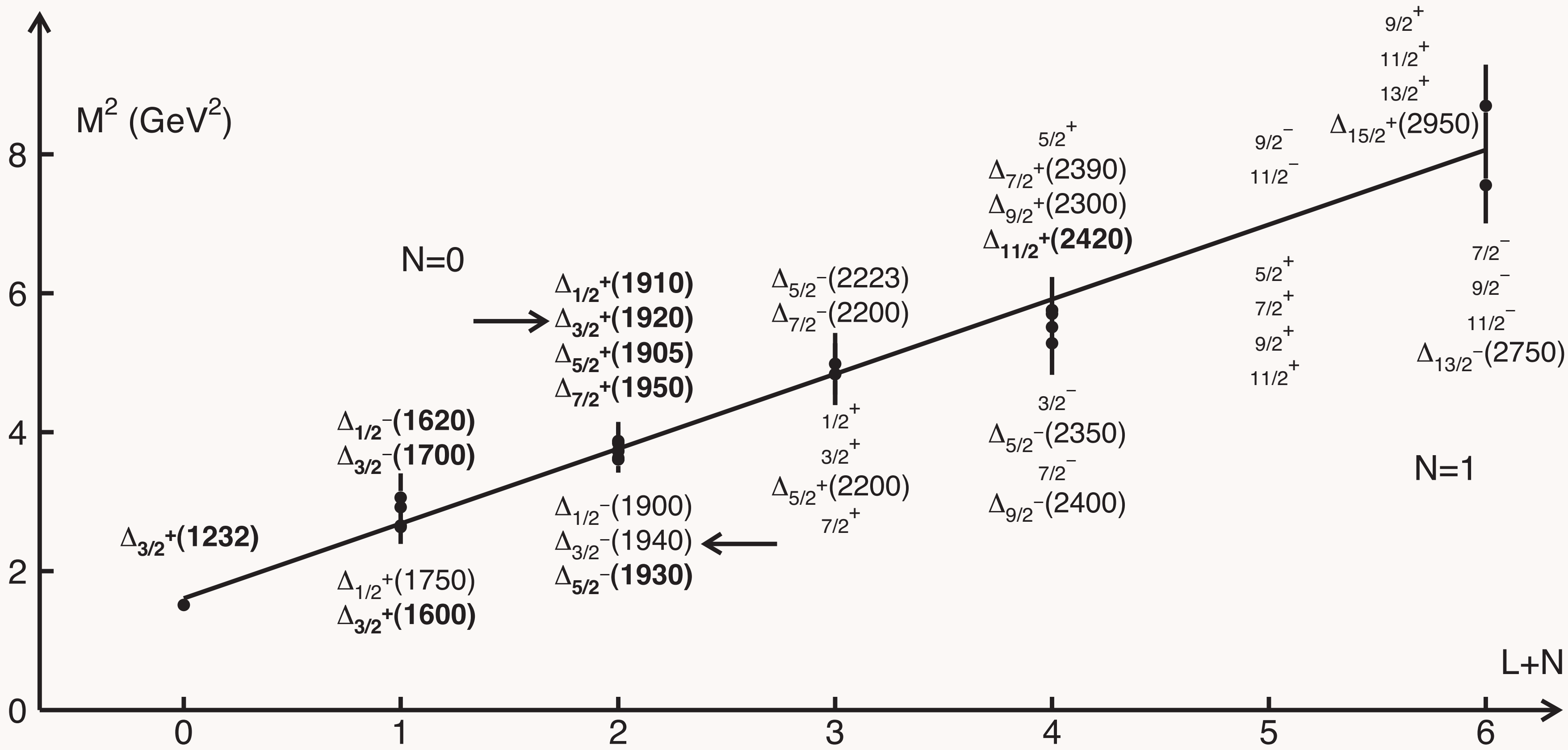

E. Klempt *et al.*: Δ^* resonances, quark models, chiral symmetry and AdS/QCD

H. Forkel, M. Beyer and T. Frederico, JHEP **0707** (2007) 077.
H. Forkel, M. Beyer and T. Frederico, Int. J. Mod. Phys. E **16** (2007) 2794.

Space-Like Dirac Proton Form Factor

- Consider the spin non-flip form factors

$$F_+(Q^2) = g_+ \int d\zeta\, J(Q,\zeta) |\psi_+(\zeta)|^2,$$
$$F_-(Q^2) = g_- \int d\zeta\, J(Q,\zeta) |\psi_-(\zeta)|^2,$$

where the effective charges g_+ and g_- are determined from the spin-flavor structure of the theory.

- Choose the struck quark to have $S^z = +1/2$. The two AdS solutions $\psi_+(\zeta)$ and $\psi_-(\zeta)$ correspond to nucleons with $J^z = +1/2$ and $-1/2$.

- For $SU(6)$ spin-flavor symmetry

$$F_1^p(Q^2) = \int d\zeta\, J(Q,\zeta) |\psi_+(\zeta)|^2,$$
$$F_1^n(Q^2) = -\frac{1}{3} \int d\zeta\, J(Q,\zeta) \left[|\psi_+(\zeta)|^2 - |\psi_-(\zeta)|^2 \right],$$

where $F_1^p(0) = 1,\ F_1^n(0) = 0$.

- Scaling behavior for large Q^2: $Q^4 F_1^p(Q^2) \to \text{constant}$ $\boxed{\text{Proton } \tau = 3}$

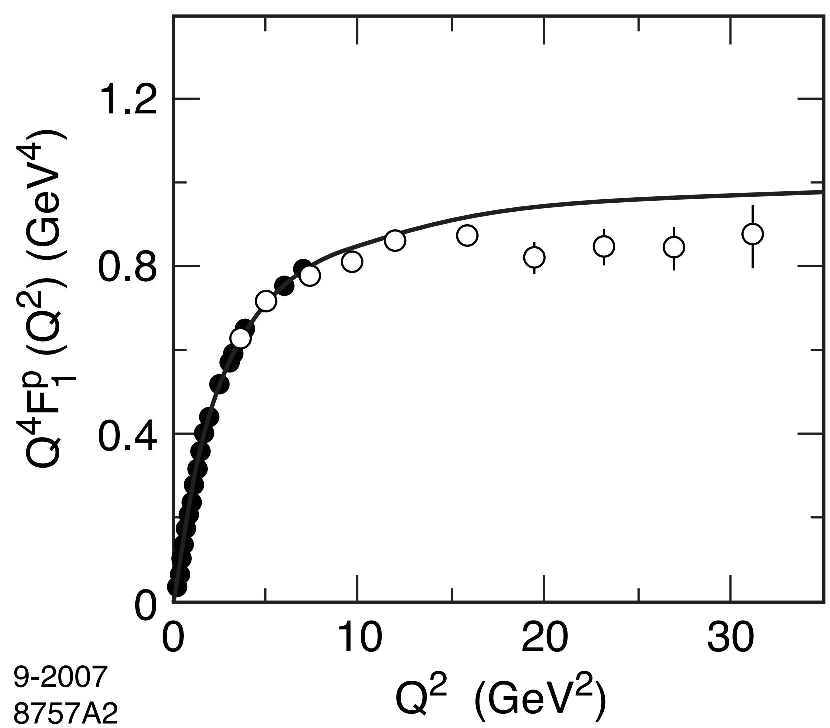

SW model predictions for $\kappa = 0.424$ GeV. Data analysis from: M. Diehl *et al.* Eur. Phys. J. C **39**, 1 (2005).

- Scaling behavior for large Q^2: $Q^4 F_1^n(Q^2) \rightarrow \text{constant}$ $\boxed{\text{Neutron } \tau = 3}$

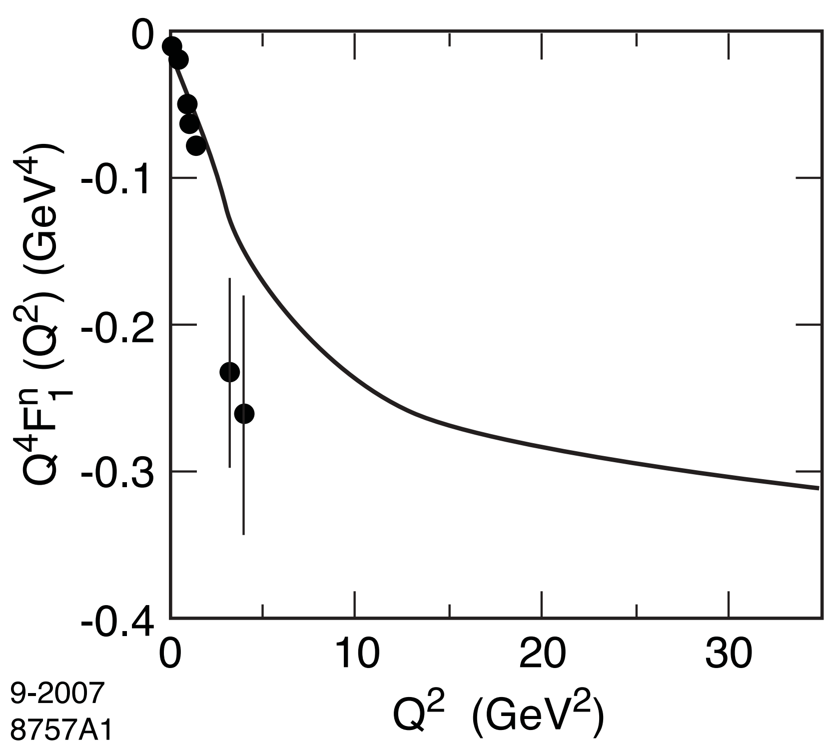

SW model predictions for $\kappa = 0.424$ GeV. Data analysis from M. Diehl *et al.* Eur. Phys. J. C **39**, 1 (2005).

Dirac Neutron Form Factor

(Valence Approximation)

Truncated Space Confinement

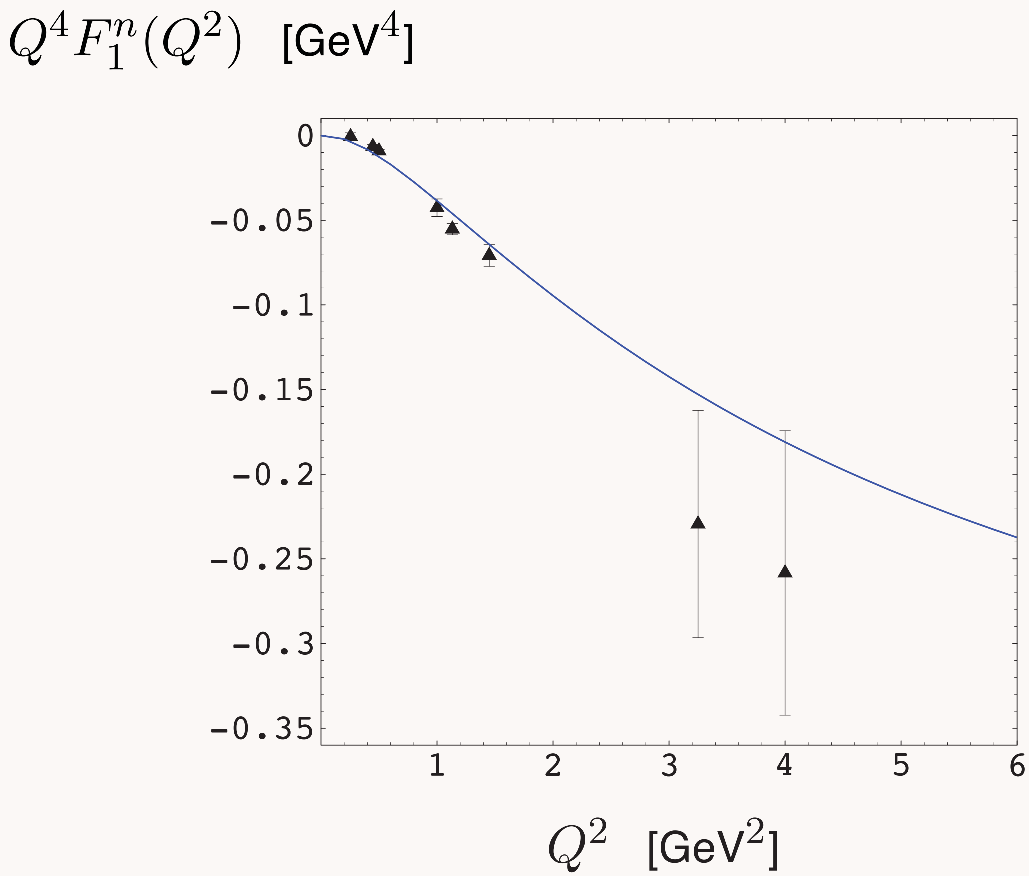

Prediction for $Q^4 F_1^n(Q^2)$ for $\Lambda_{\rm QCD} = 0.21$ GeV in the hard wall approximation. Data analysis from Diehl (2005).

Spacelike Pauli Form Factor

Preliminary

From overlap of $L = 1$ and $L = 0$ LFWFs

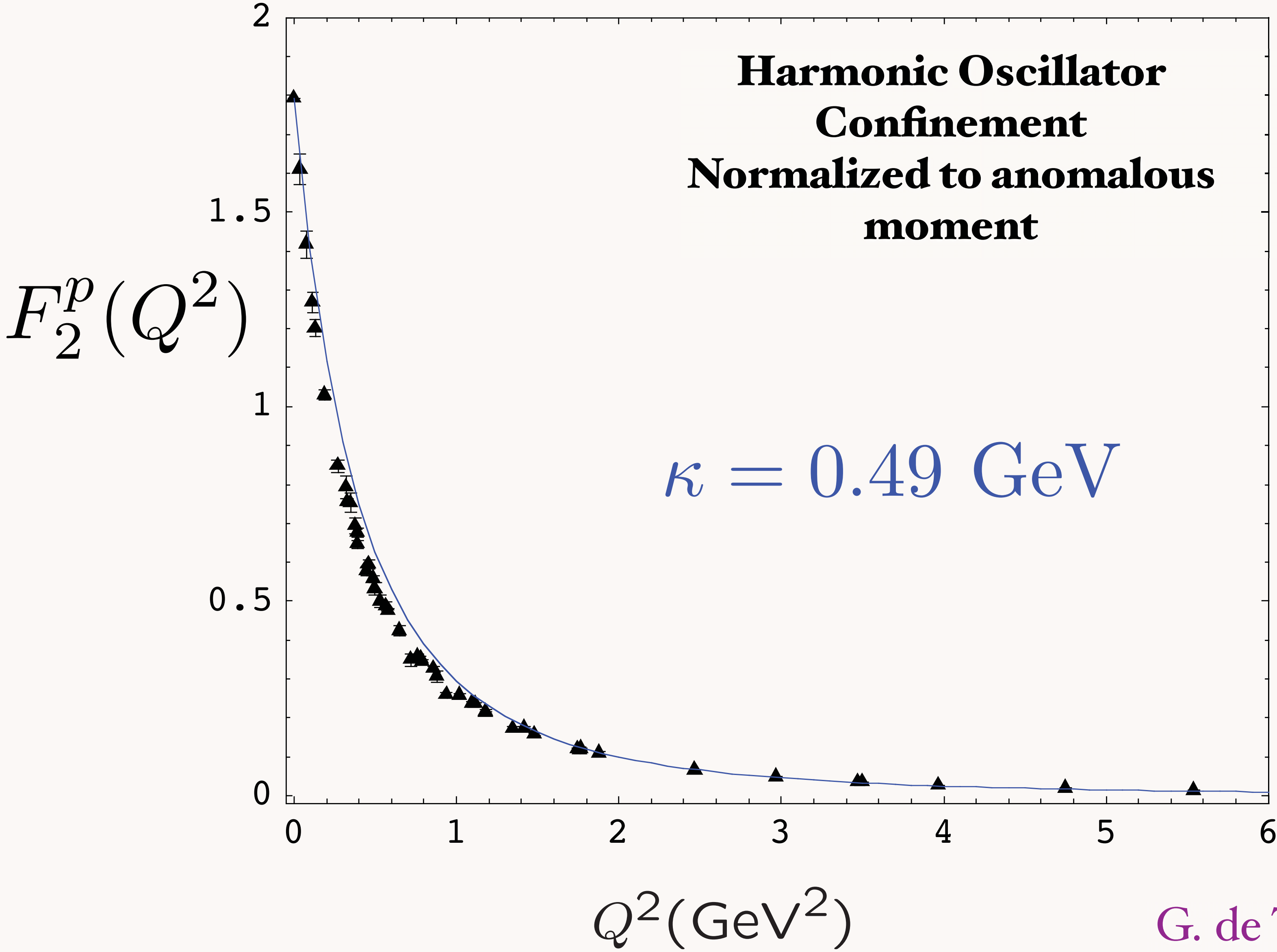

G. de Teramond, sjb

LF(3+1) $\longleftrightarrow$ AdS$_5$

$$\psi(x, \vec{b}_\perp) \quad \longleftrightarrow \quad \phi(z)$$

$$\zeta = \sqrt{x(1-x)\vec{b}_\perp^2} \quad \longleftrightarrow \quad z$$

$\psi(x, \vec{b}_\perp)$

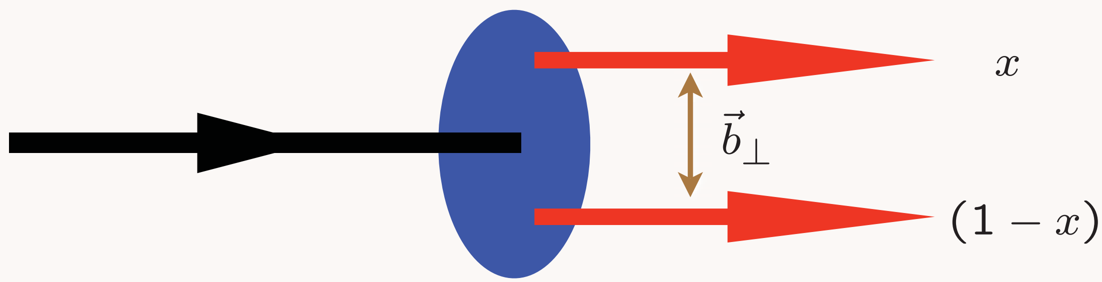

$$\psi(x, \vec{b}_\perp) = \sqrt{\frac{x(1-x)}{2\pi\zeta}}\,\phi(\zeta)$$

Light-Front Holography: Unique mapping derived from equality of LF and AdS formula for current matrix elements

$$\left[-\frac{d^2}{d\zeta^2} + V(\zeta)\right]\phi(\zeta) = \mathcal{M}^2\phi(\zeta)$$

de Teramond, sjb

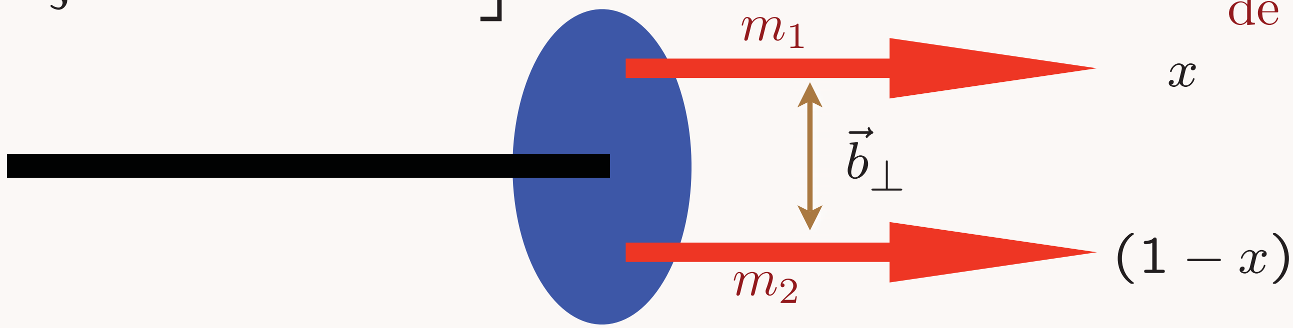

$$\zeta = \sqrt{x(1-x)\vec{b}_\perp^2}$$ *Holographic Variable*

$$-\frac{d}{d\zeta^2} \equiv \frac{k_\perp^2}{x(1-x)}$$ *LF Kinetic Energy in momentum space*

Assume LFWF is a dynamical function of the quark-antiquark invariant mass squared

$$-\frac{d}{d\zeta^2} \rightarrow -\frac{d}{d\zeta^2} + \frac{m_1^2}{x} + \frac{m_2^2}{1-x} \equiv \frac{k_\perp^2 + m_1^2}{x} + \frac{k_\perp^2 + m_2^2}{1-x}$$

Result: Soft-Wall LFWF for massive constituents

$$\psi(x,\mathbf{k}_\perp) = \frac{4\pi c}{\kappa\sqrt{x(1-x)}} e^{-\frac{1}{2\kappa^2}\left(\frac{\mathbf{k}_\perp^2}{x(1-x)}+\frac{m_1^2}{x}+\frac{m_2^2}{1-x}\right)}$$

LF WF in impact space: soft-wall model with massive quarks

$$\psi(x,\mathbf{b}_\perp) = \frac{c\,\kappa}{\sqrt{\pi}}\sqrt{x(1-x)}\, e^{-\frac{1}{2}\kappa^2 x(1-x)\mathbf{b}_\perp^2 - \frac{1}{2\kappa^2}\left[\frac{m_1^2}{x}+\frac{m_2^2}{1-x}\right]}$$

$$z \to \zeta \to \chi$$

$$\chi^2 = b^2 x(1-x) + \frac{1}{\kappa^4}\left[\frac{m_1^2}{x} + \frac{m_2^2}{1-x}\right]$$

J/ψ

LFWF peaks at

$$x_i = \frac{m_{\perp i}}{\sum_j^n m_{\perp j}}$$

where

$$m_{\perp i} = \sqrt{m^2 + k_\perp^2}$$

minimum of LF energy denominator

$$\kappa = 0.375 \text{ GeV}$$

$$\psi_{J/\psi}(x, b)$$

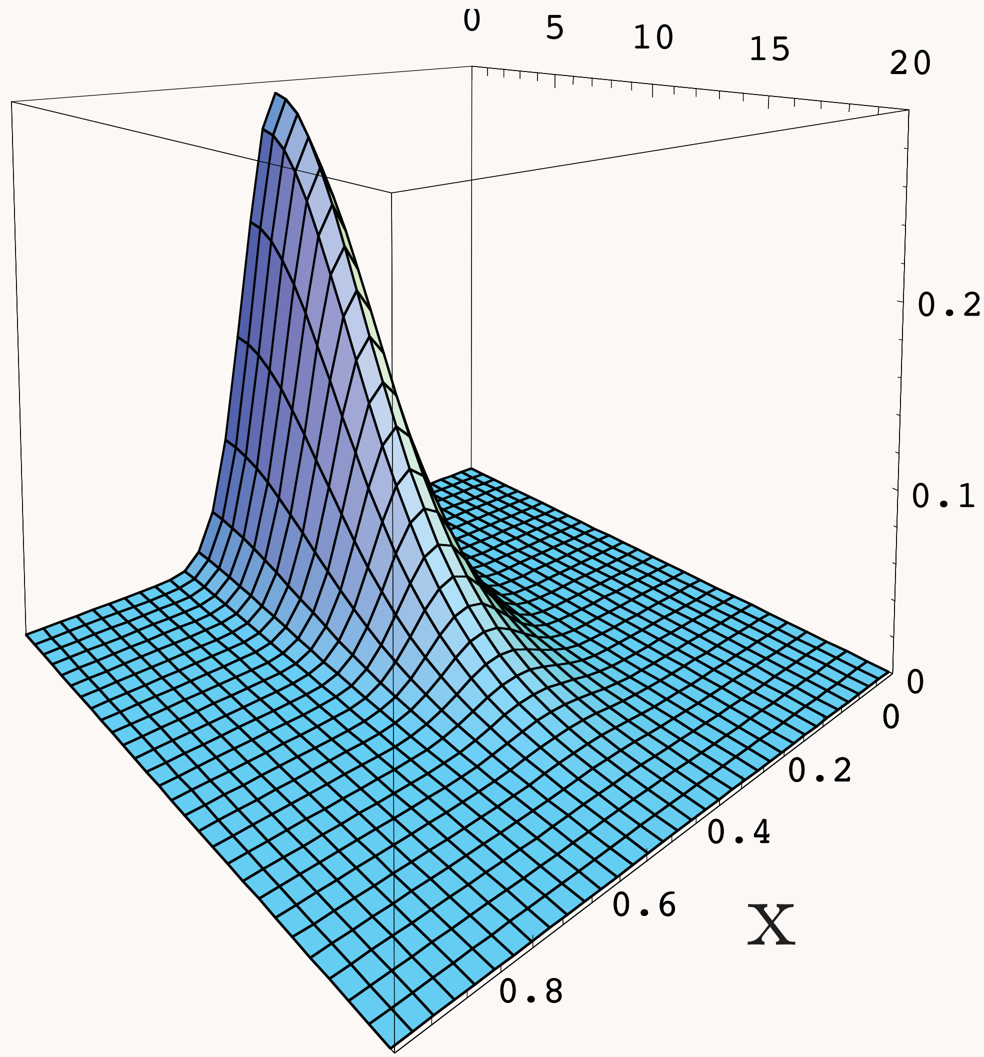

$$m_a = m_b = 1.25 \text{ GeV}$$

$|\pi^+ >= |u\bar{d} >$

$m_u = 2\ MeV$
$m_d = 5\ MeV$

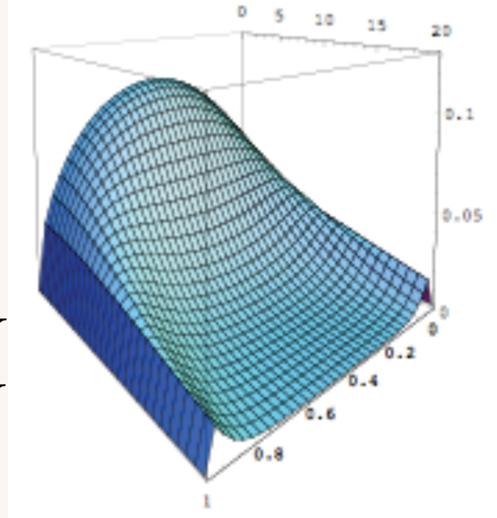

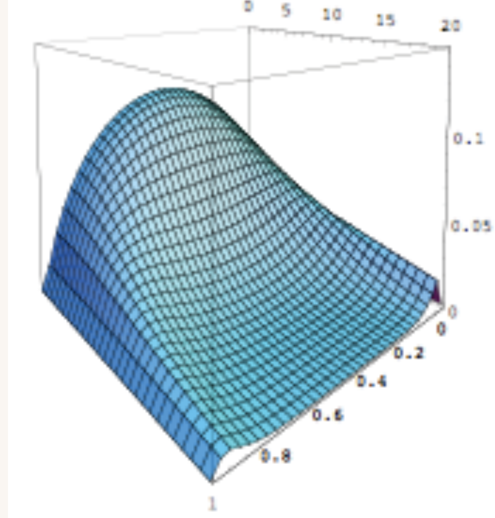

$|K^+ >= |u\bar{s} >$

$m_s = 95\ MeV$

$|D^+ >= |c\bar{d} >$

$m_c = 1.25\ GeV$

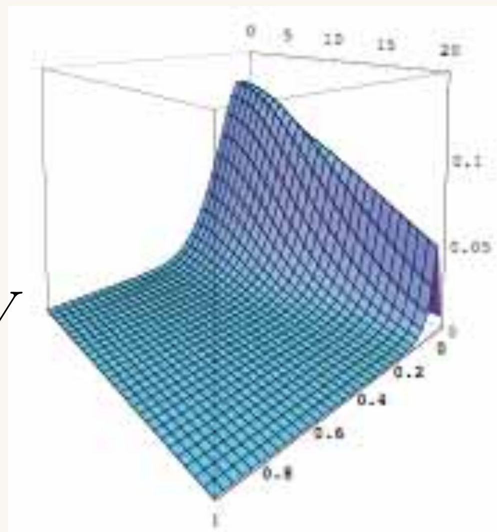

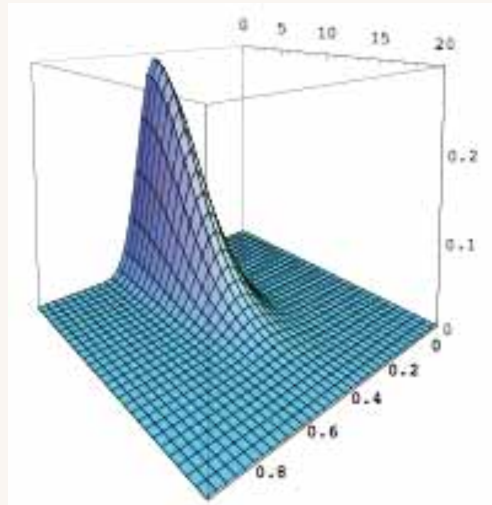

$|\eta_c >= |c\bar{c} >$

$|B^+ >= |u\bar{b} >$

$m_b = 4.2\ GeV$

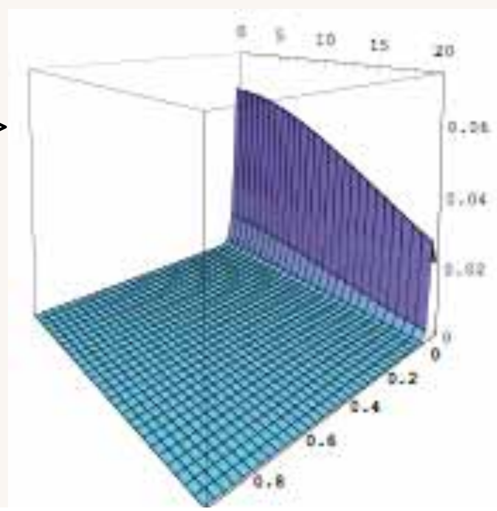

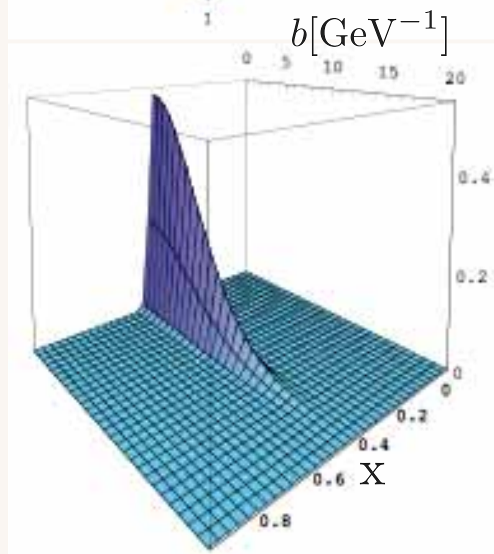

$|\eta_b >= |b\bar{b} >$

$\kappa = 375\ MeV$

First Moment of Kaon Distribution Amplitude

$$< \xi > = \int_{-1}^{1} d\xi \; \xi \; \phi(\xi)$$

$$\xi = 1 - 2x$$

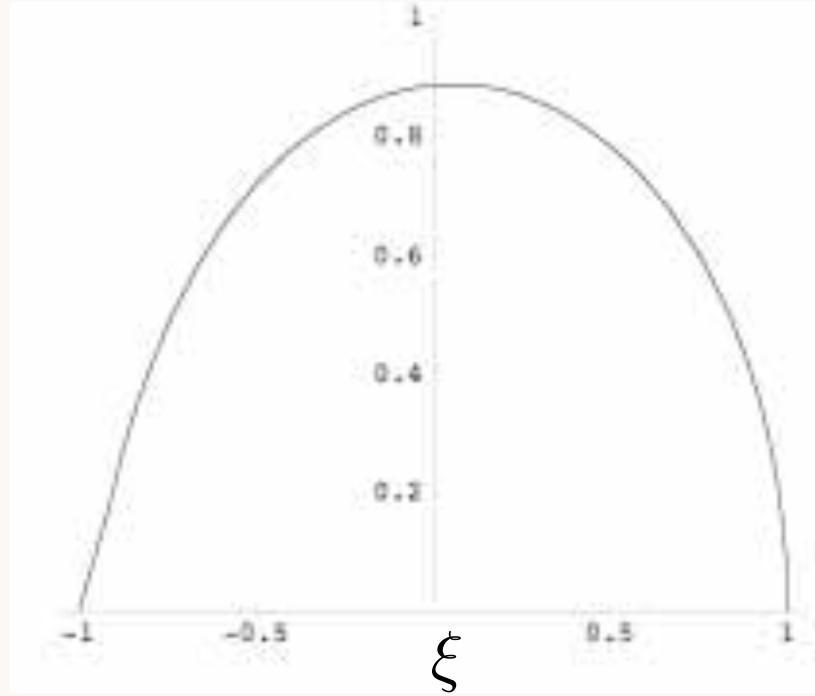

$$< \xi >_K = 0.04 \pm 0.02 \qquad \kappa = 375 \; MeV$$

Range from $m_s = 65 \pm 25$ MeV (PDG)

$< \xi >_K = 0.029 \; \pm 0.002$ Donnellan et al.

$< \xi >_K = 0.0272 \pm 0.0005$ Braun et al.

Hadronization at the Amplitude Level

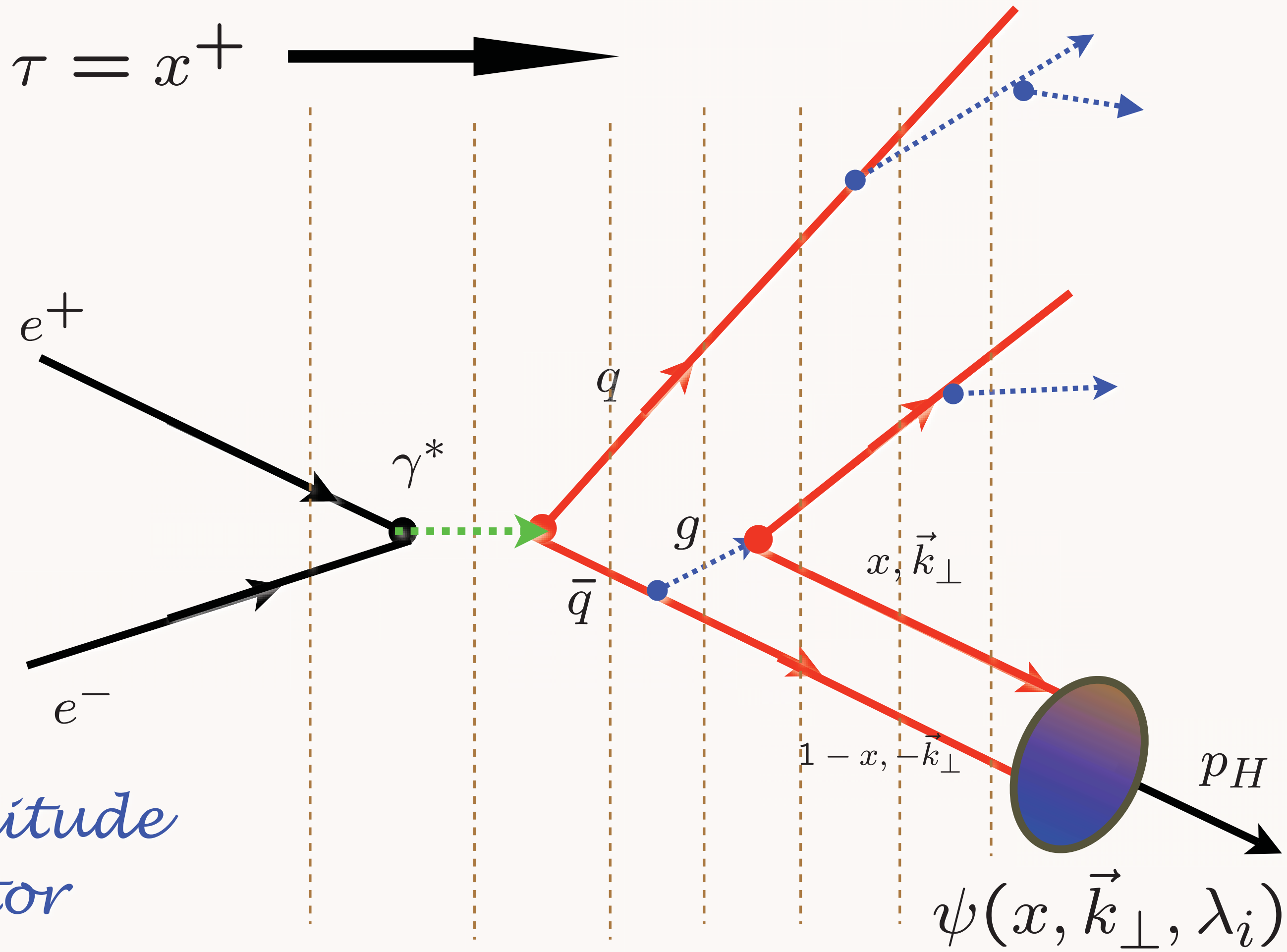

Event amplitude generator

Construct helicity amplitude using Light-Front Perturbation theory; coalesce quarks via LFWFs

Hadronization at the Amplitude Level

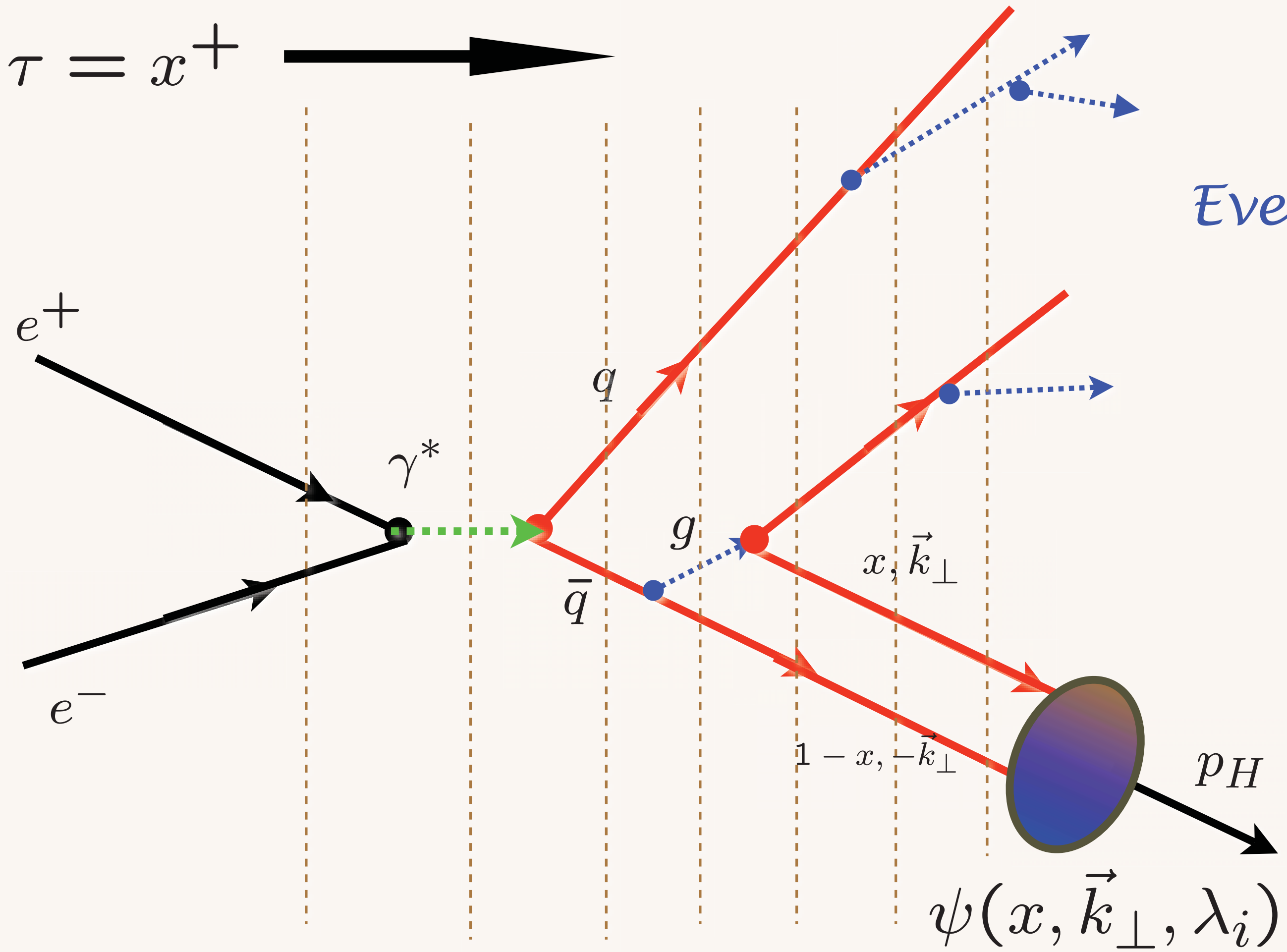

Event amplitude generator

AdS/QCD Hard Wall Confinement:

Capture if $\zeta^2 = x(1-x)b_\perp^2 > \frac{1}{\Lambda^2_{QCD}}$

i.e.,

$\mathcal{M}^2 = \frac{k_\perp^2}{x(1-x)} < \Lambda^2_{QCD}$

Use AdS/CFT orthonormal LFWFs as a basis for diagonalizing the QCD LF Hamiltonian

- Good initial approximant
- Better than plane wave basis

Pauli, Hornbostel, Hiller, McCartor, sjb

- DLCQ discretization -- highly successful 1+1
- Use independent HO LFWFs, remove CM motion

Vary, Harinandrath, Maris, sjb

- Similar to Shell Model calculations

Light-Front QCD Heisenberg Equation

$$H_{LC}^{QCD}|\Psi_h\rangle = \mathcal{M}_h^2\, |\Psi_h\rangle$$

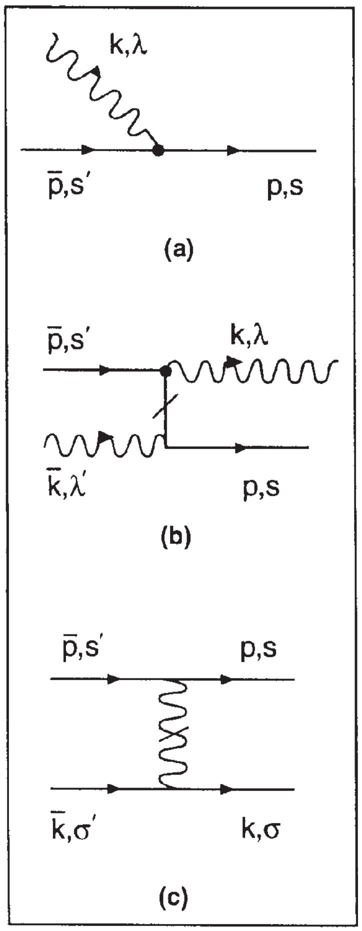

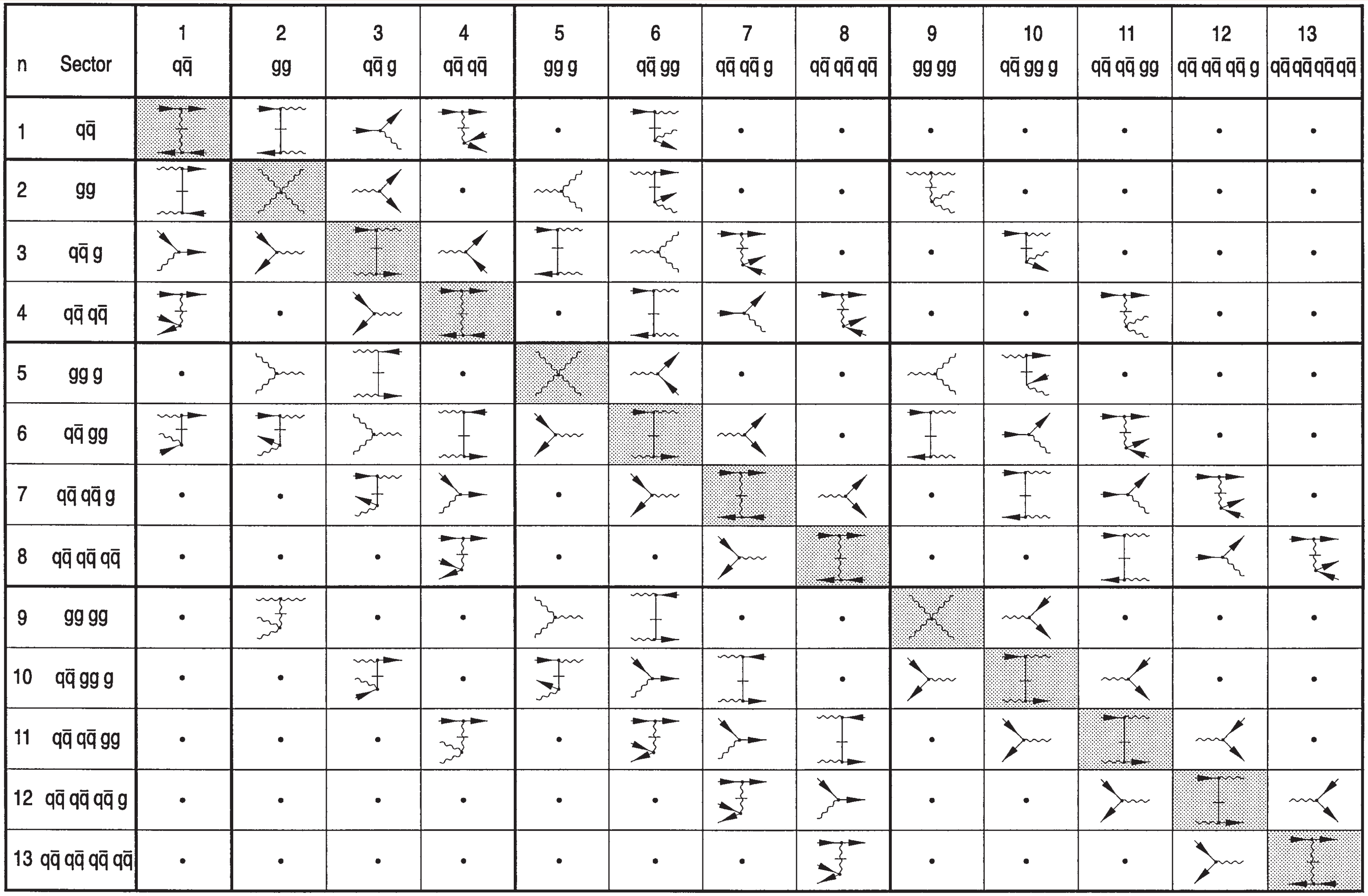

Use AdS/QCD basis functions

$$\Delta M_p^2 = g < p_F|A^\mu \bar\psi \gamma_\mu \psi|p_I >$$

$$|p_F >= |u^+ u^+ d^- \bar d^+ d^+ >_{L^z=-1}$$

$$\simeq |(u^+ d^+ d^-)_n (u^+ \bar d^+)_{\rho_+} >_{L^z=-1}$$

$$|P_I >= |u^+ u^+ d^- g^+ >_{L^z=-1}$$

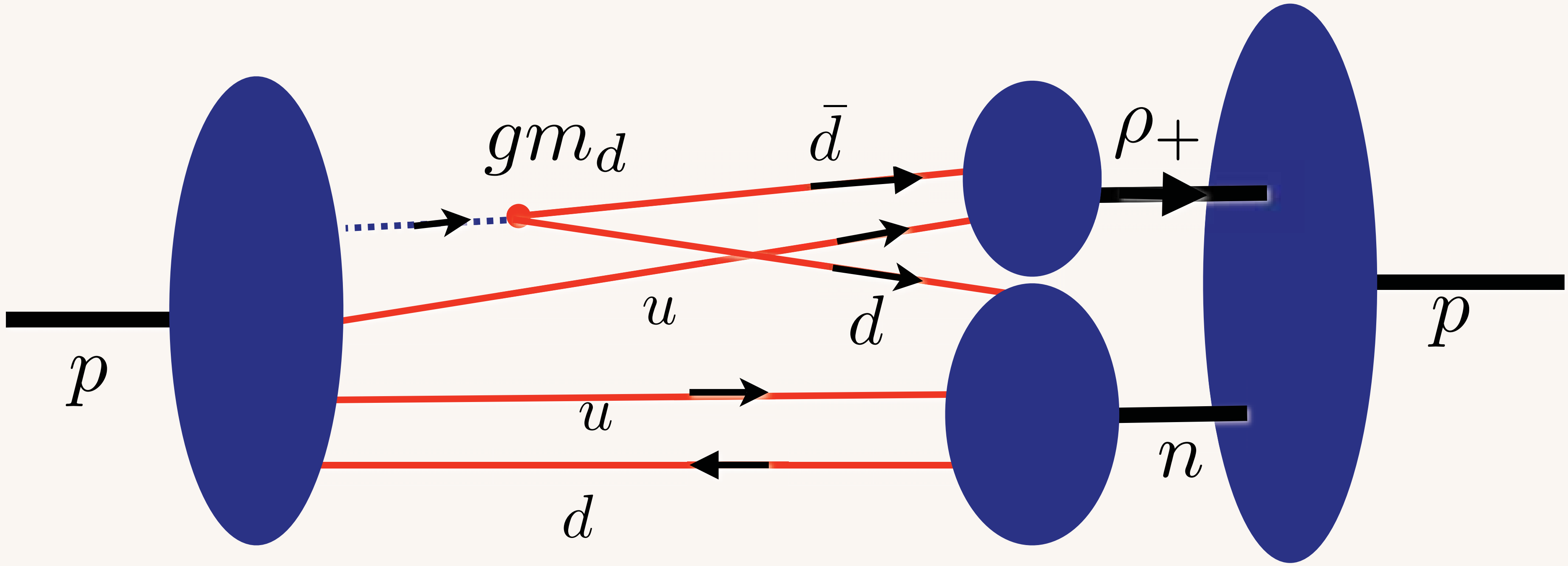

$$H_I^{LF} = gA\bar\psi\gamma^\mu\psi \sim -gm_q a_g b_q^\dagger d_q^\dagger$$

Linear quark mass term generated by transition from valence to meson-nucleon LF Fock state

Dynamical chiral symmetry breaking: Zero cosmological constant

$\pi N \to \mu^+ \mu^- X$ at high x_F

In the limit where $(1-x_F)Q^2$ is fixed as $Q^2 \to \infty$

Entire pion wf contributes to hard process

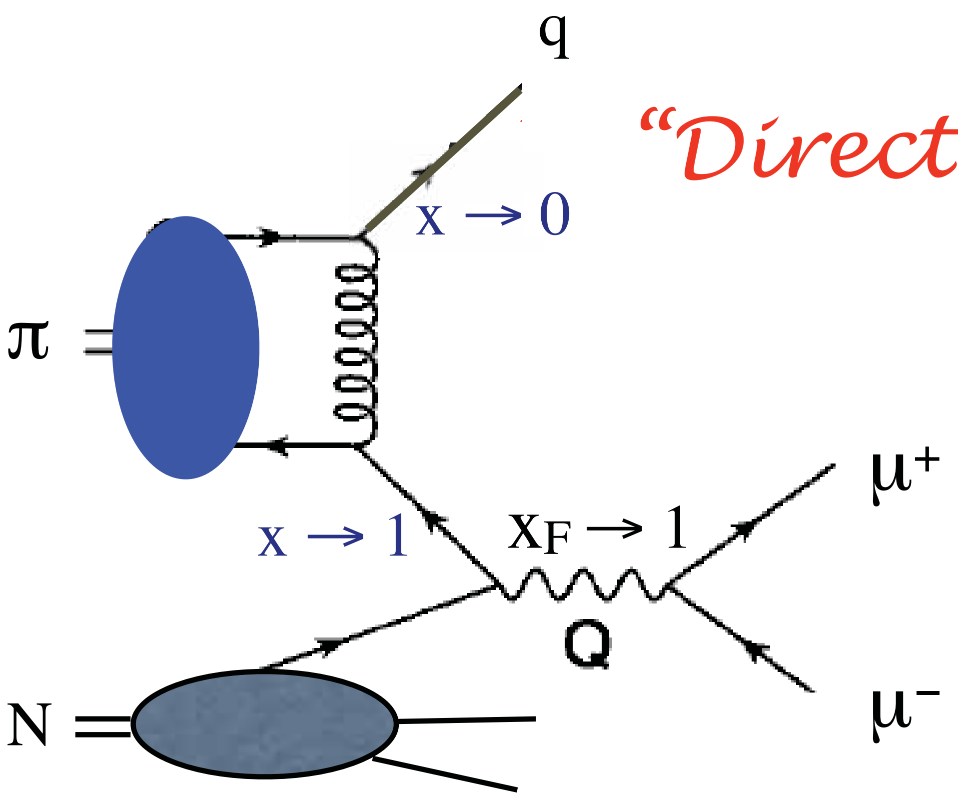

"Direct" Subprocess

Virtual photon is longitudinally polarized

Berger, sjb
Khoze, Brandenburg, Muller, sjb
Hoyer Vanttinen

$$\pi^- N \rightarrow \mu^+ \mu^- X \text{ at } 80 \text{ GeV}/c$$

$$\frac{d\sigma}{d\Omega} \propto 1 + \lambda \cos^2\theta + \rho \sin 2\theta \cos\phi + \omega \sin^2\theta \cos 2\phi.$$

$$\frac{d^2\sigma}{dx_\pi d\cos\theta} \propto x_\pi \left[(1-x_\pi)^2 (1+\cos^2\theta) + \frac{4}{9} \frac{\langle k_T^2 \rangle}{M^2} \sin^2\theta \right]$$

$$\langle k_T^2 \rangle = 0.62 \pm 0.16 \text{ GeV}^2/c^2$$

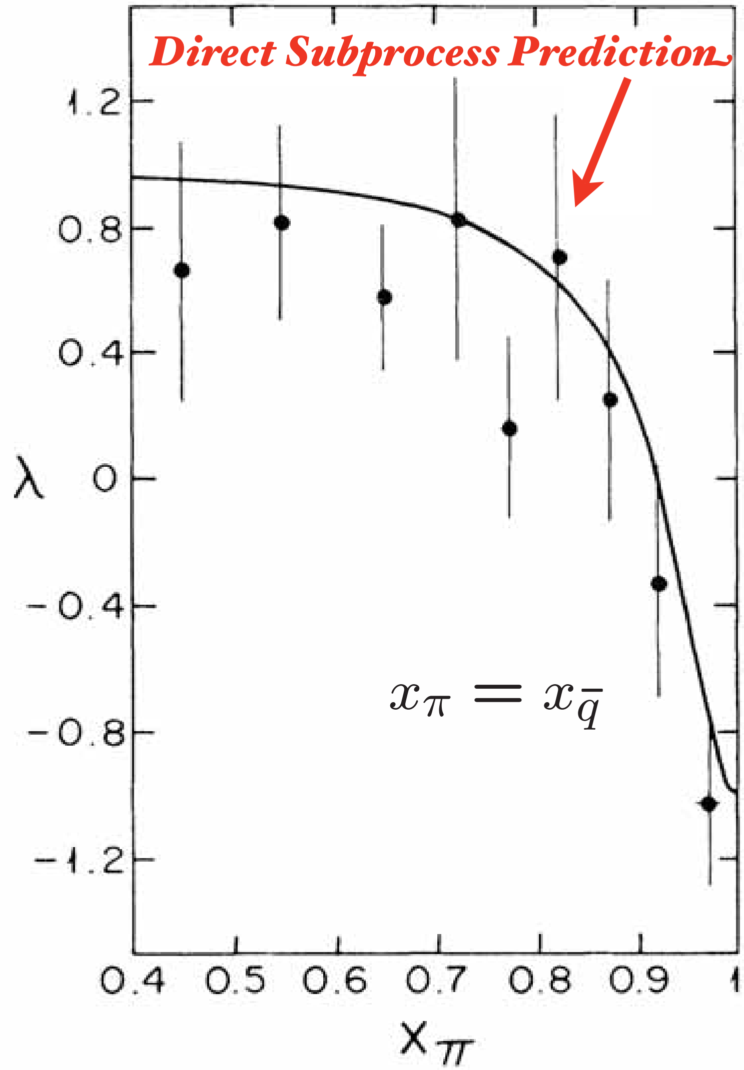

Dramatic change in angular distribution at large x_F

Chicago-Princeton Collaboration

Phys.Rev.Lett.55:2649,1985

Example of a higher-twist direct subprocess

Crucial Test of Leading -Twist QCD: Scaling at fixed x_T

$$x_T = \frac{2p_T}{\sqrt{s}}$$

$$E\frac{d\sigma}{d^3p}(pN \to \pi X) = \frac{F(x_T,\theta_{CM})}{p_T^{neff}}$$

Parton model: $n_{eff} = 4$

As fundamental as Bjorken scaling in DIS

Conformal scaling: $n_{eff} = 2\, n_{active} - 4$

$\sqrt{s}^n E \frac{d\sigma}{d^3p}(pp \to \gamma X)$ at fixed x_T

Tannenbaum

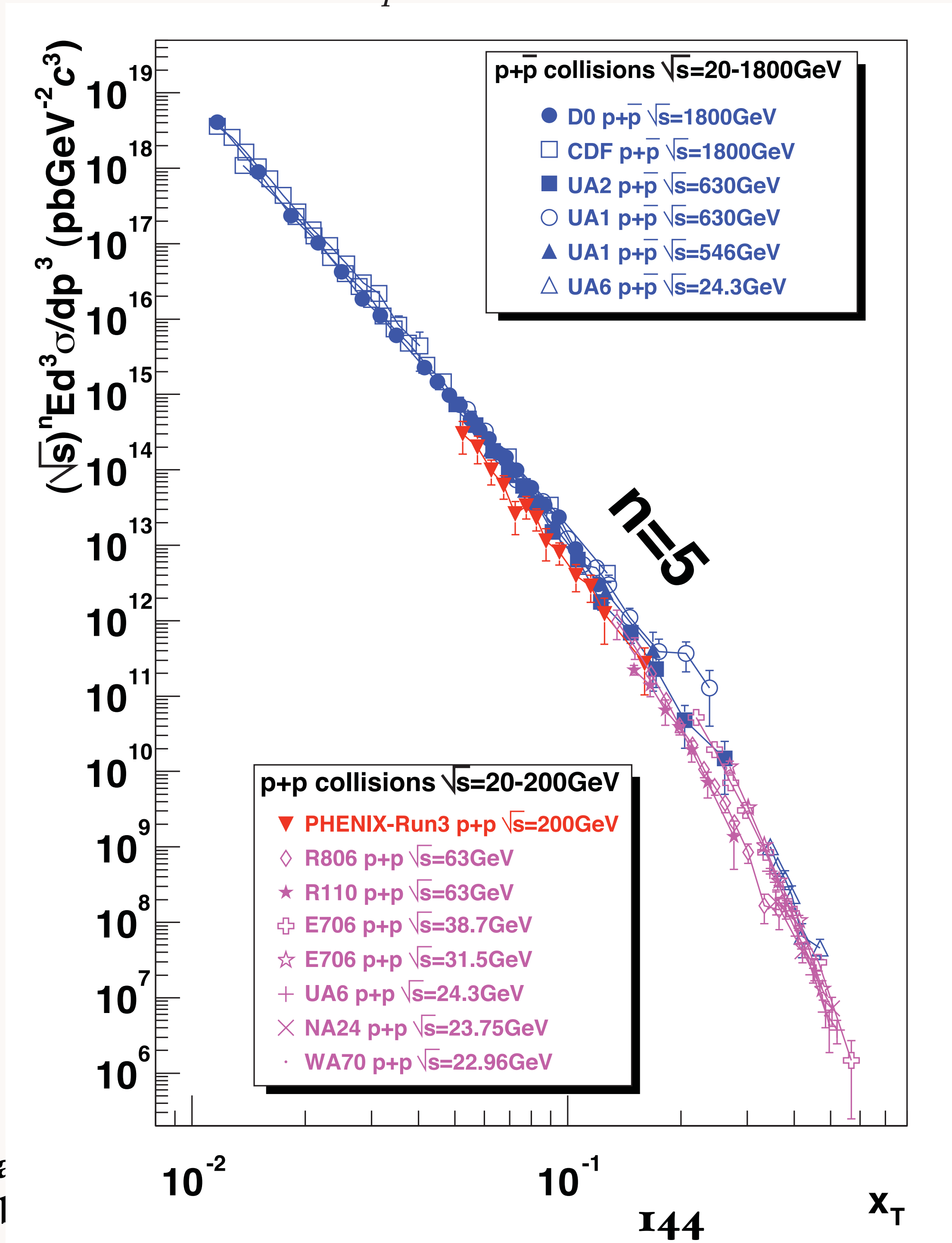

Scaling of direct photon production consistent with PQCD

$pp \longrightarrow \gamma X$

$$E\frac{d\sigma}{d^3p}(pp \to \gamma X) = \frac{F(\theta_{cm}, x_T)}{p_T^4}$$

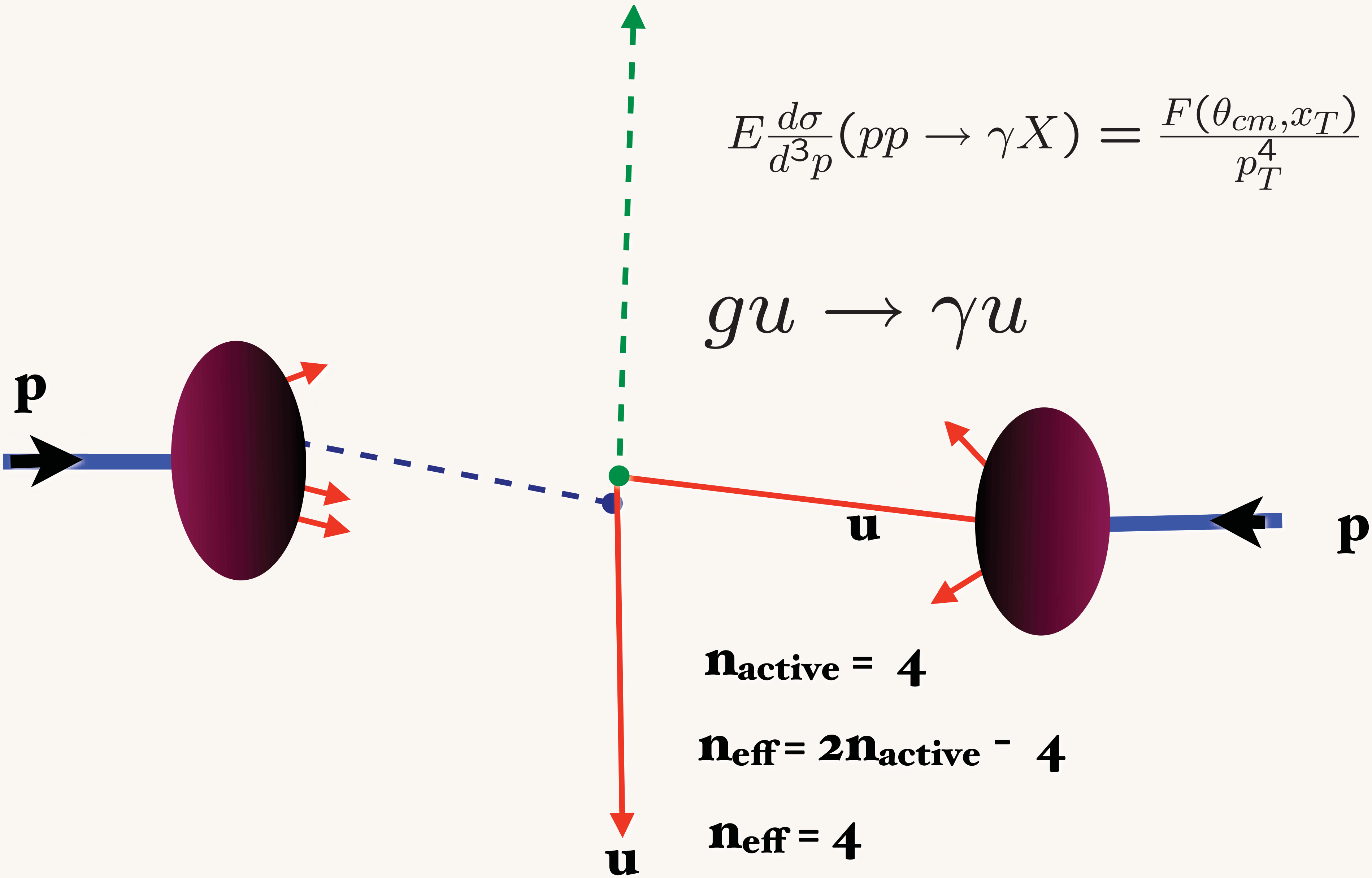

QCD prediction: Modification of power fall-off due to DGLAP evolution and the Running Coupling

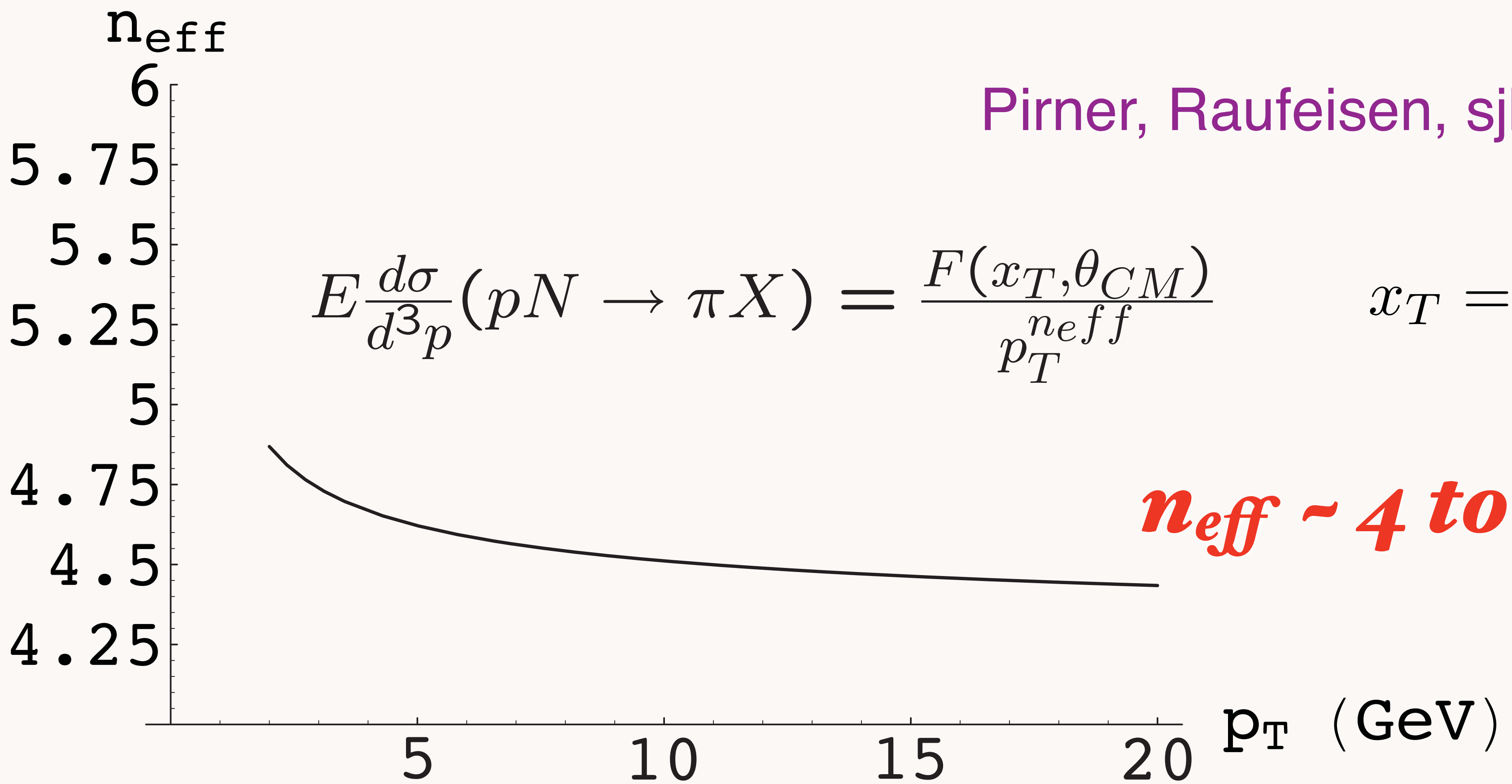

Pirner, Raufeisen, sjb

$$E\frac{d\sigma}{d^3p}(pN \to \pi X) = \frac{F(x_T, \theta_{CM})}{p_T^{n_{eff}}} \qquad x_T = \frac{2p_T}{\sqrt{s}}$$

$n_{eff} \sim 4$ to 5

Key test of PQCD: power-law fall-off at fixed x_T

$$E\frac{d\sigma}{d^3p}(pp \to HX) = \frac{F(x_T, \theta_{cm} = \pi/2)}{p_T^{n_{eff}}}$$

$n_{\rm eff}$

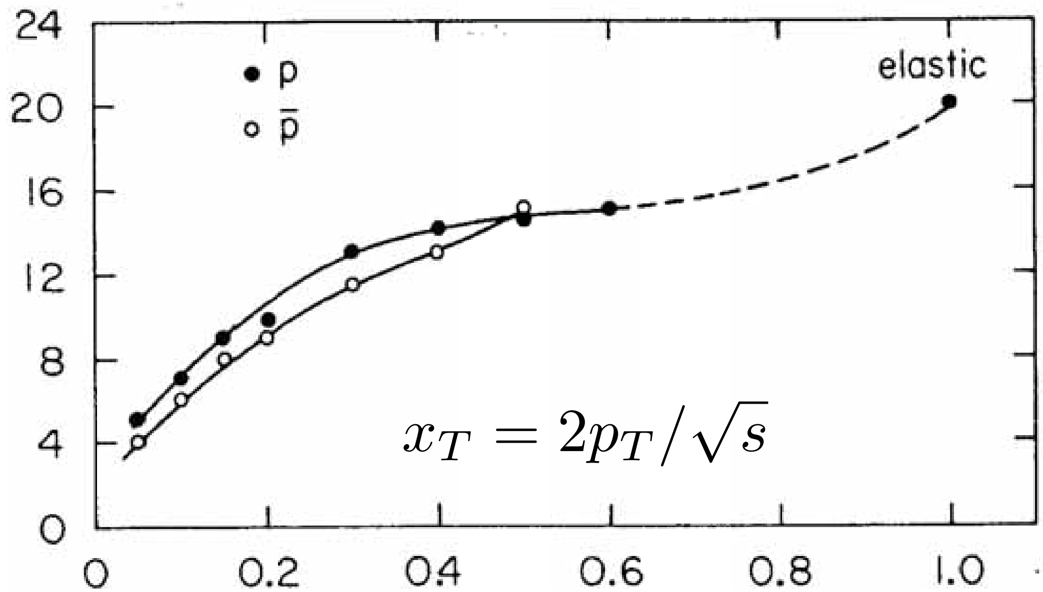

Clear evidence for higher-twist contributions

Fermilab, ISR data

$n_{\rm eff}$

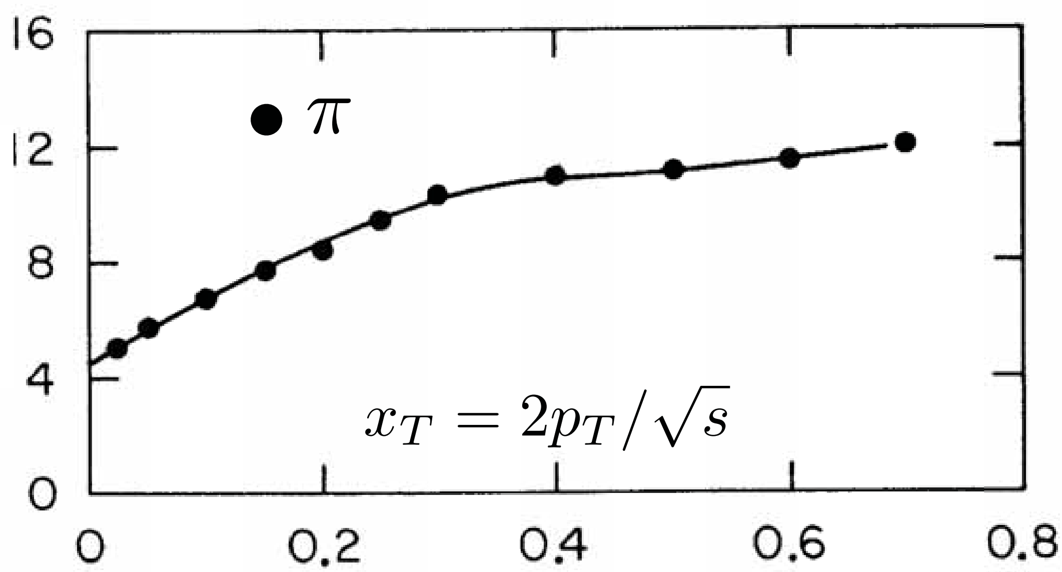

Continuous Rise of n_{eff}

$\sqrt{s}^{6.3} \times E\frac{d\sigma}{d^3p}(pp \to H^{\pm}X)$ at fixed x_T

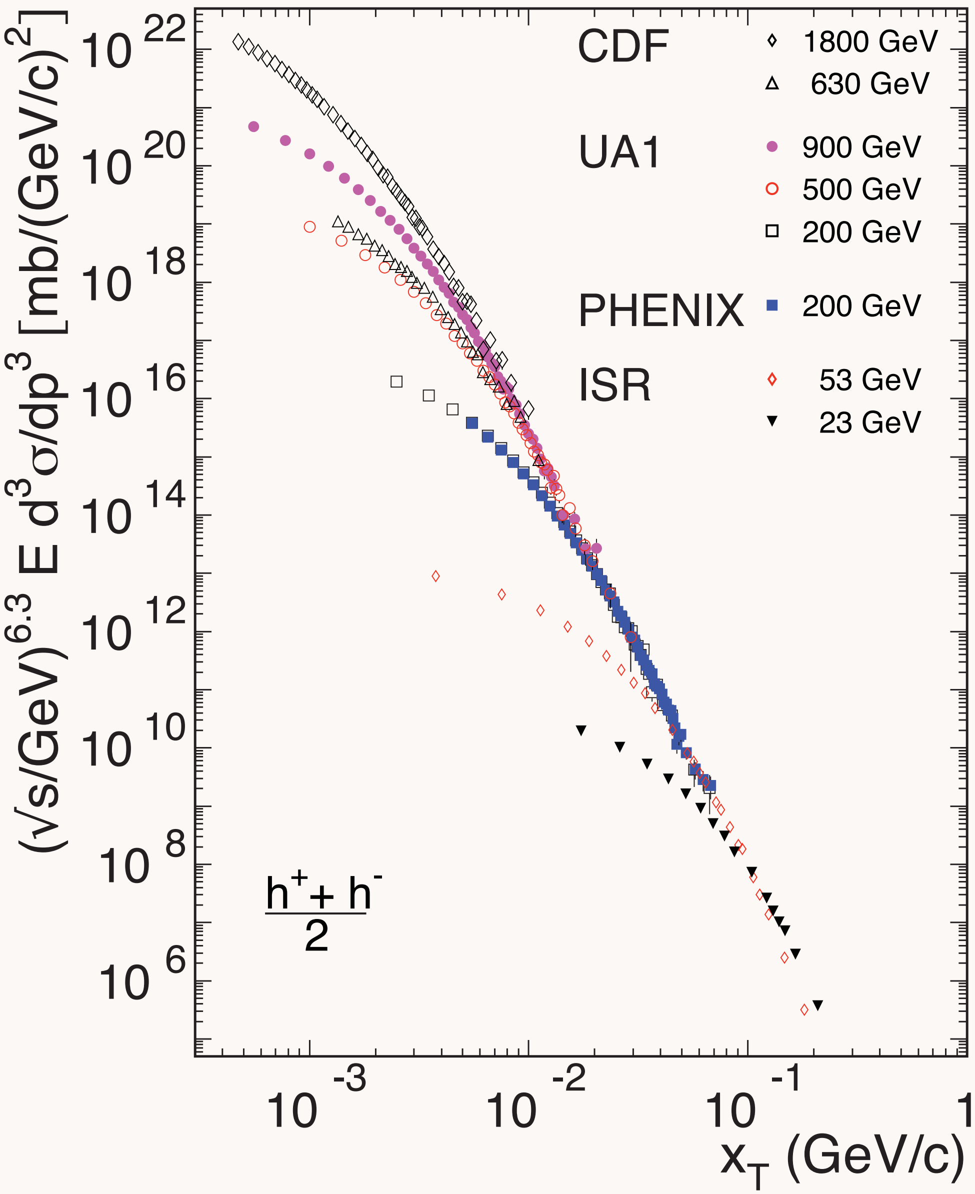

Tannenbaum

Scaling inconsistent with PQCD

Protons produced in AuAu collisions at RHIC do not exhibit clear scaling properties in the available p_T range. Shown are data for central $(0-5\%)$ and for peripheral $(60-90\%)$ collisions.

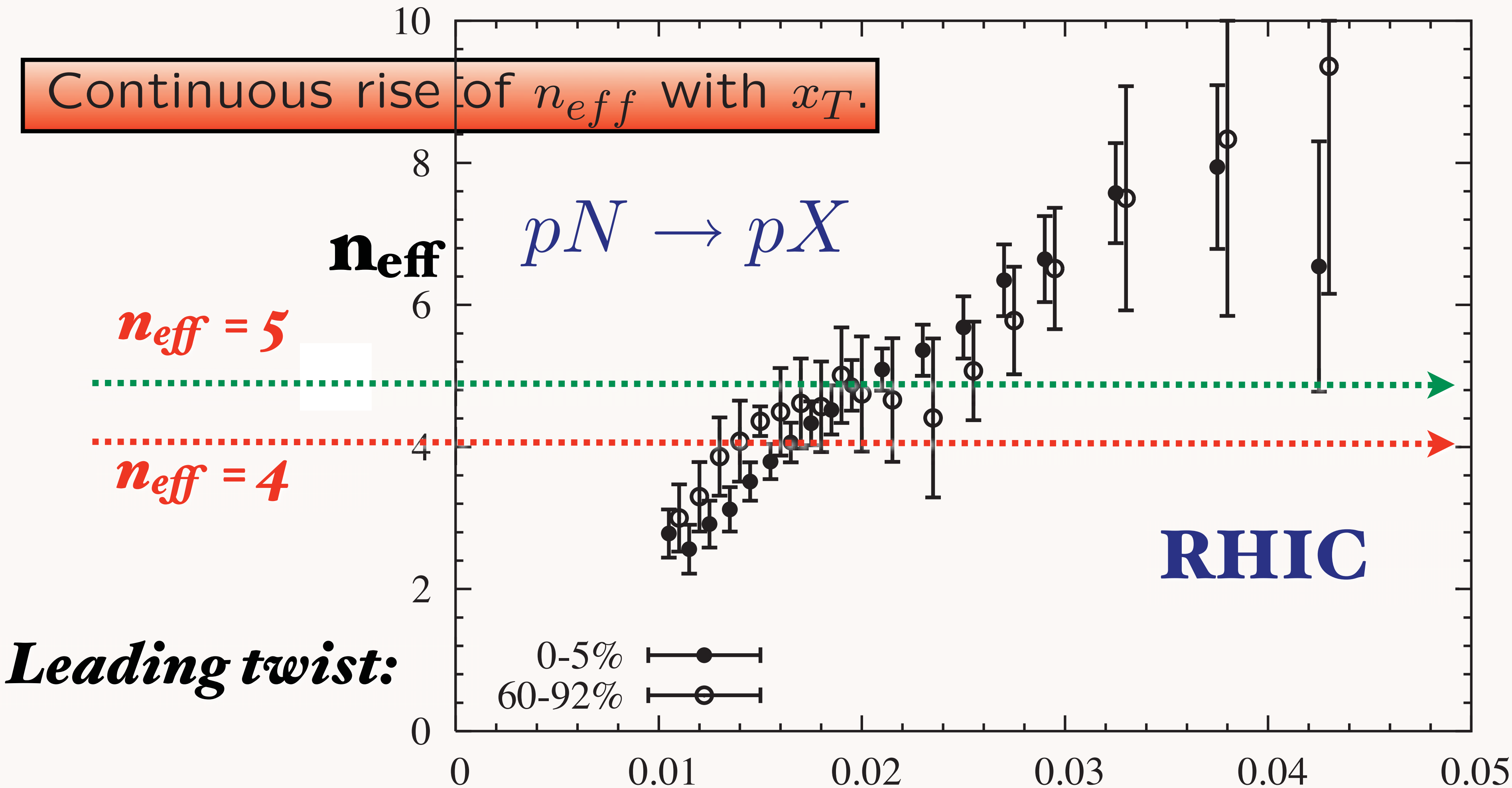

$$E\frac{d\sigma}{d^3p}(pN \to pX) = \frac{F(x_T,\theta_{CM})}{p_T^{n_{eff}}}$$

S. S. Adler *et al.* PHENIX Collaboration *Phys. Rev. Lett.* **91**, 172301 (2003).

Baryon Anomaly: Particle ratio changes with centrality!

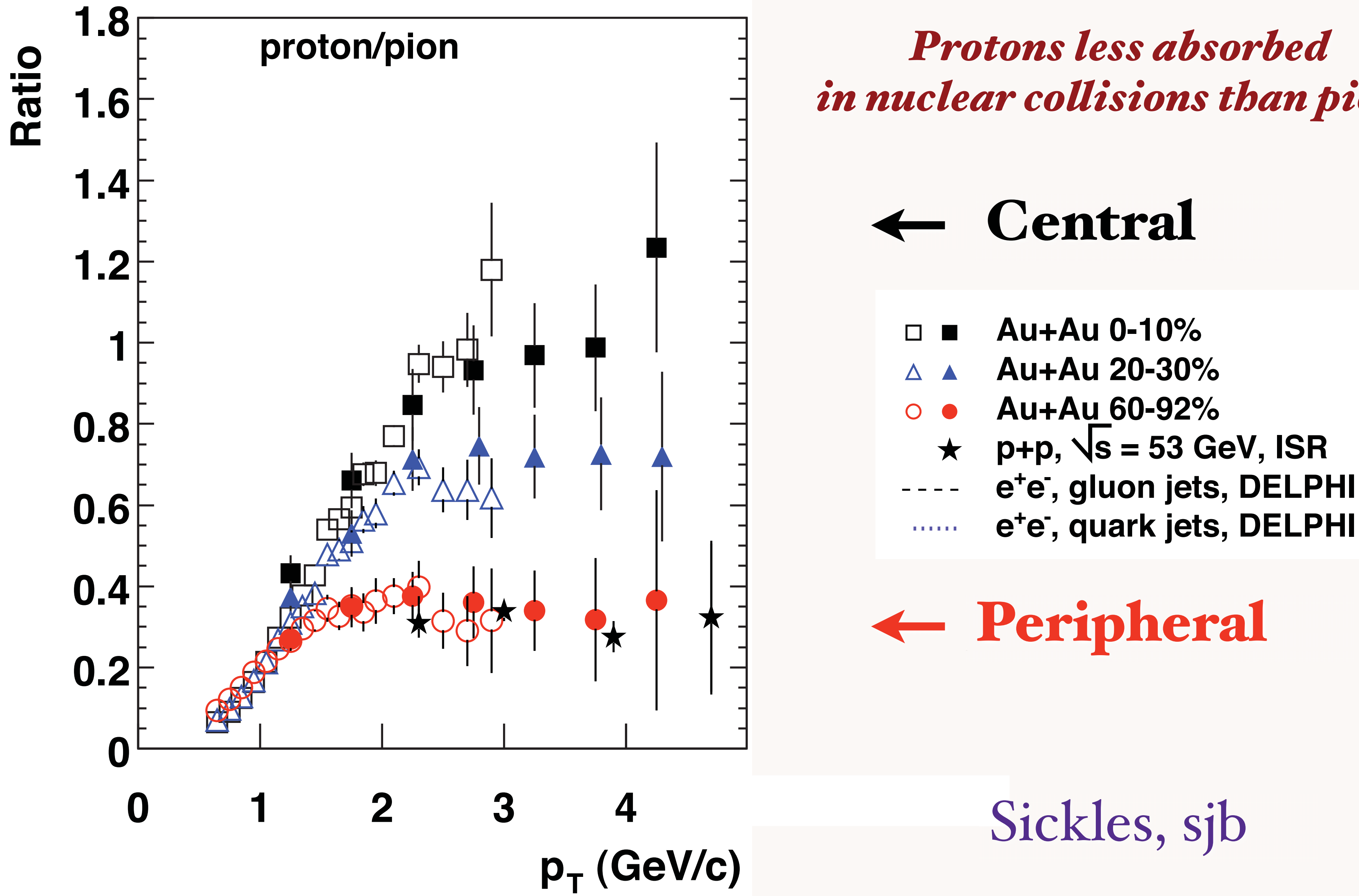

Protons less absorbed in nuclear collisions than pions

← **Central**

← **Peripheral**

Sickles, sjb

$$\sqrt{s_{NN}} = 130 \text{ and } 200 \text{ GeV}$$

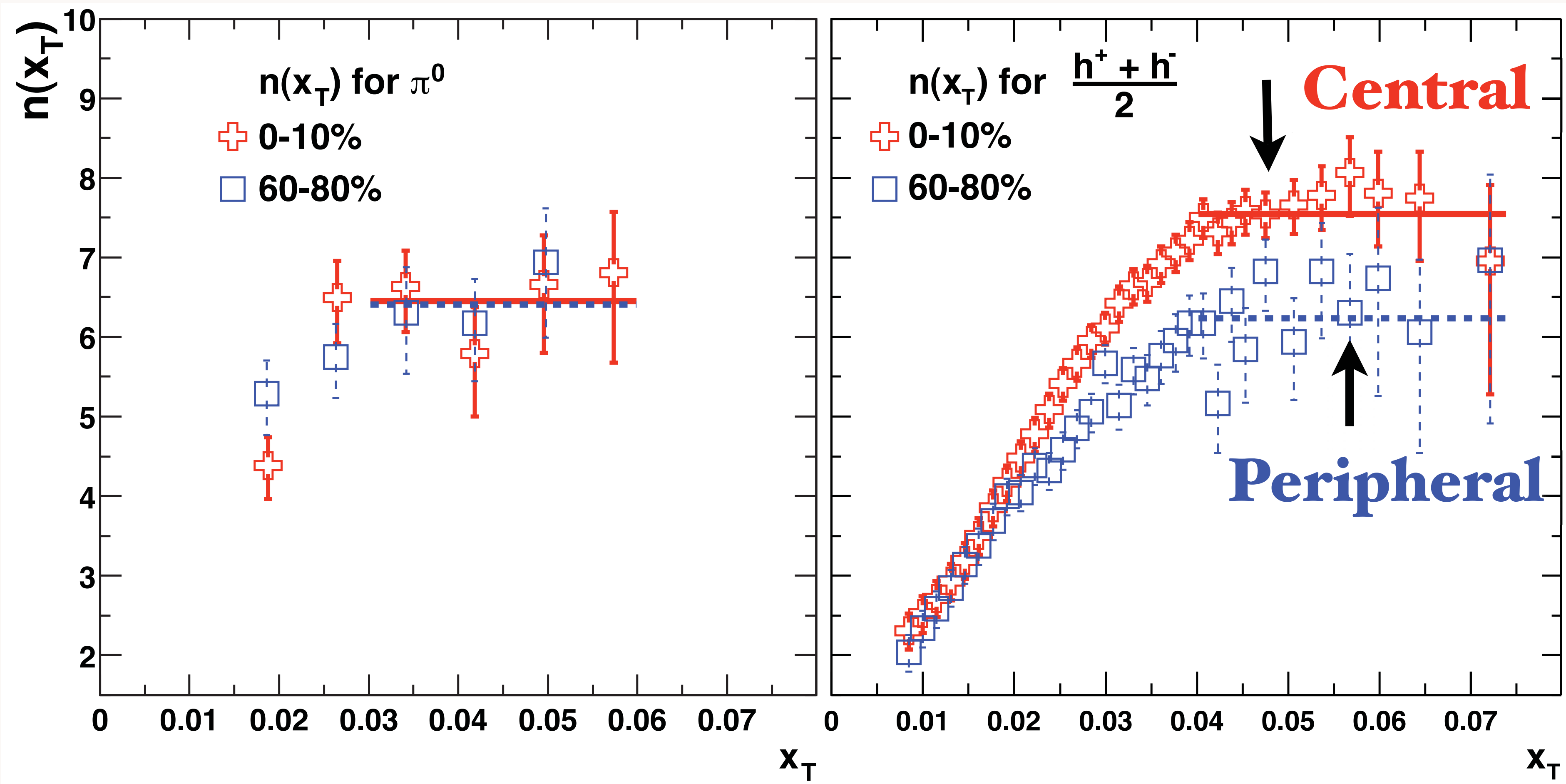

Proton power changes with centrality !

$pp \to HX$ at high p_T

Proton created from jet fragmentation

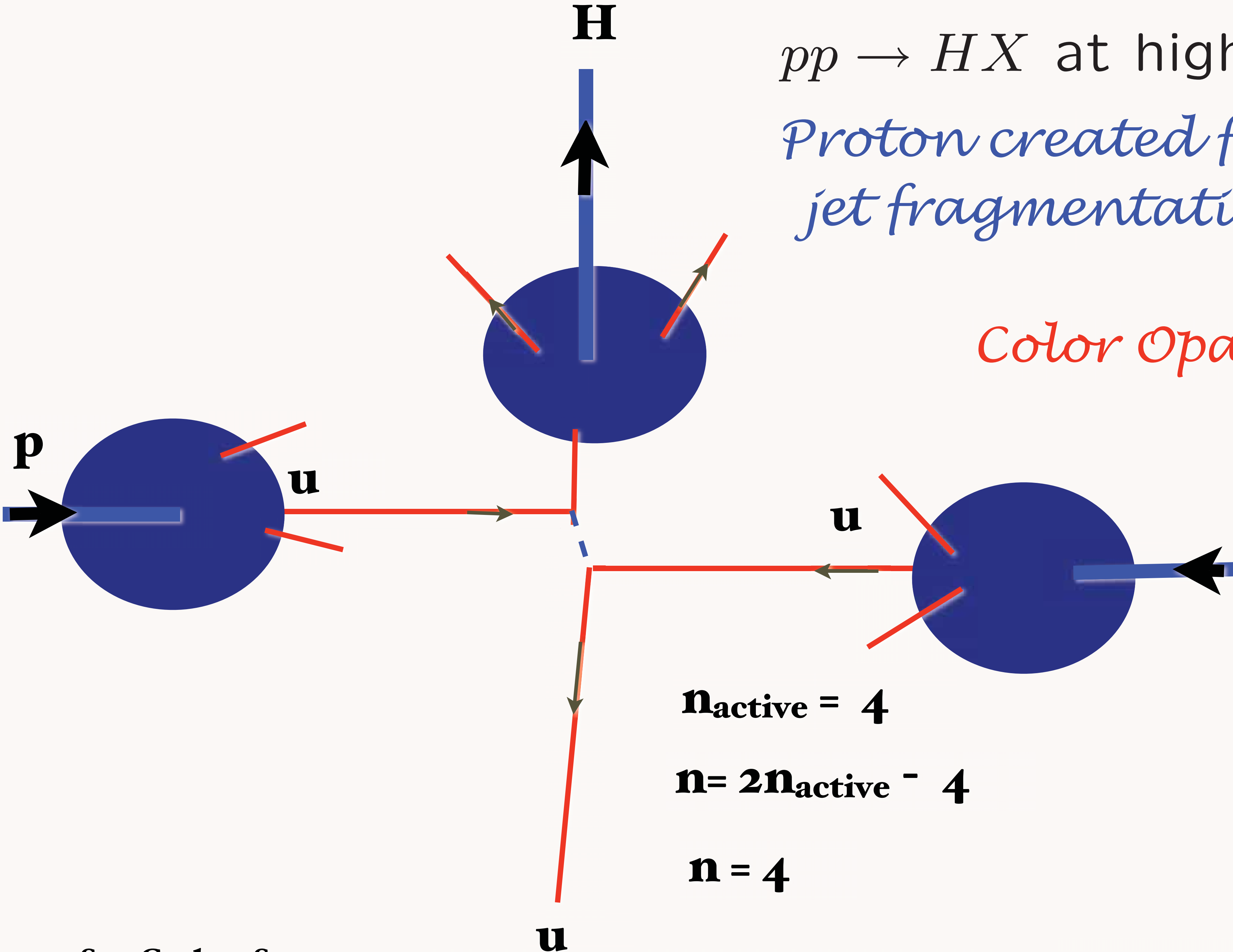

Color Opaque

$n_{active} = 4$

$n = 2n_{active} - 4$

$n = 4$

Baryon can be made directly within hard subprocess

Coalescence within hard subprocess

$$b_\perp \simeq 1/p_T$$

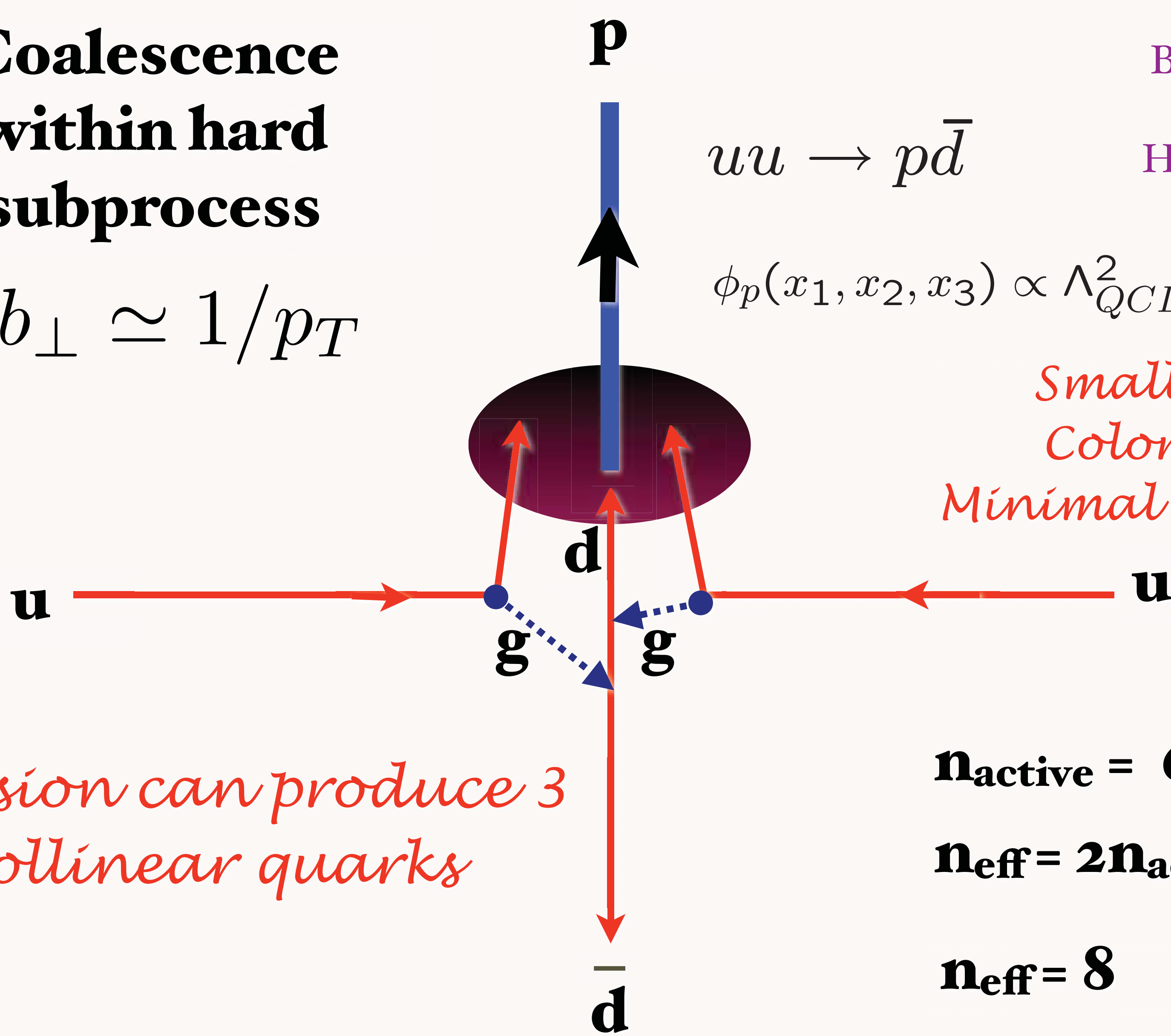

$$uu \to p\bar{d}$$

$$\phi_p(x_1, x_2, x_3) \propto \Lambda^2_{QCD}$$

Bjorken
Blankenbecler, Gunion, sjb
Berger, sjb
Hoyer, et al: Semi-Exclusive

Sickles, sjb

Small color-singlet
Color Transparent
Minimal same-side energy

Collision can produce 3 collinear quarks

n_{active} = 6

$n_{eff} = 2n_{active} - 4$

n_{eff} = 8

Baryon made directly within hard subprocess

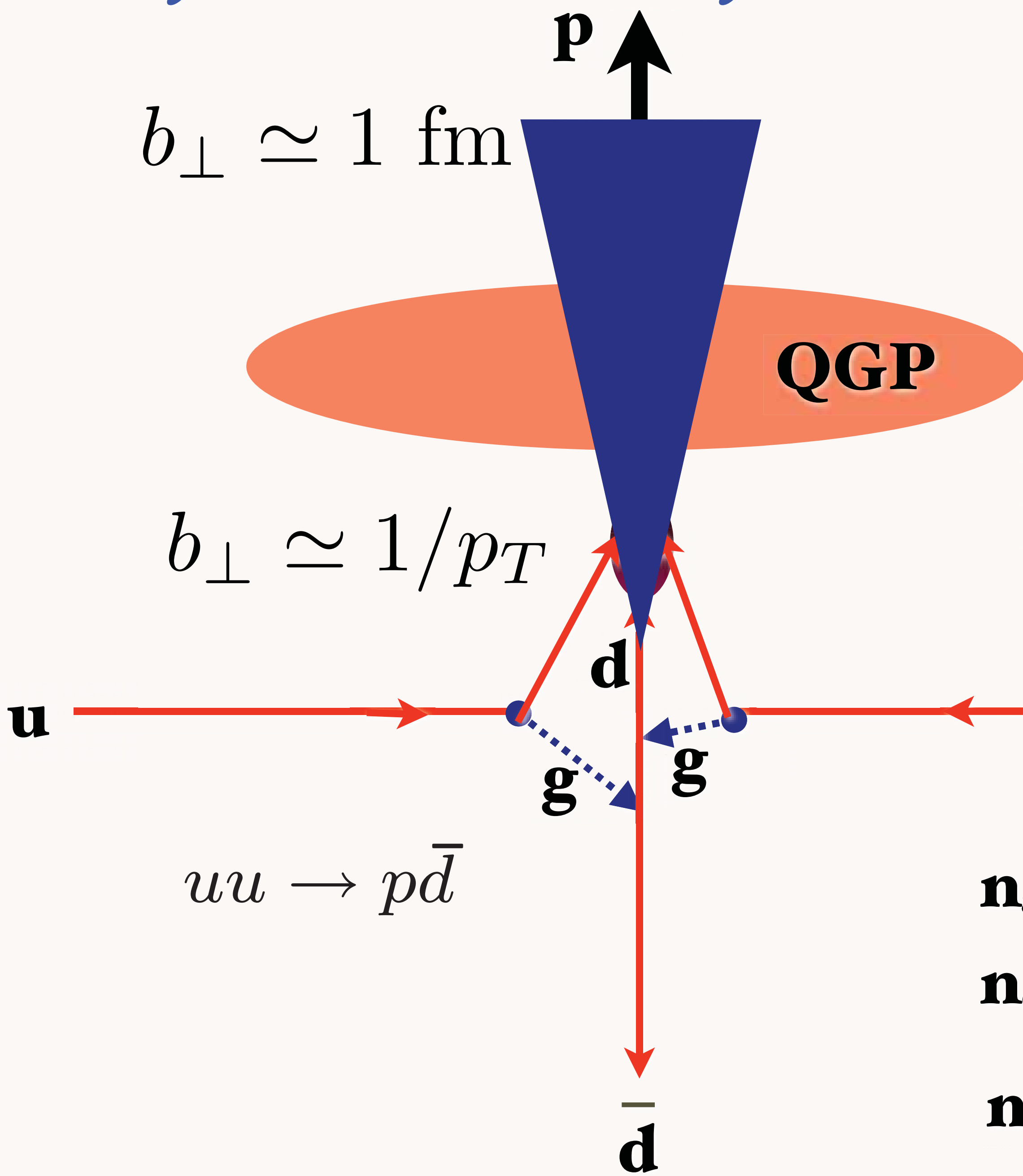

Formation Time proportional to Energy

Small color-singlet
Color Transparent
Minimal same-side energy

$n_{active} = 6$

$n_{eff} = 2n_{active} - 4$

$n_{eff} = 8$

S. S. Adler *et al*. PHENIX Collaboration *Phys. Rev. Lett*. **91**, 172301 (2003).

Particle ratio changes with centrality!

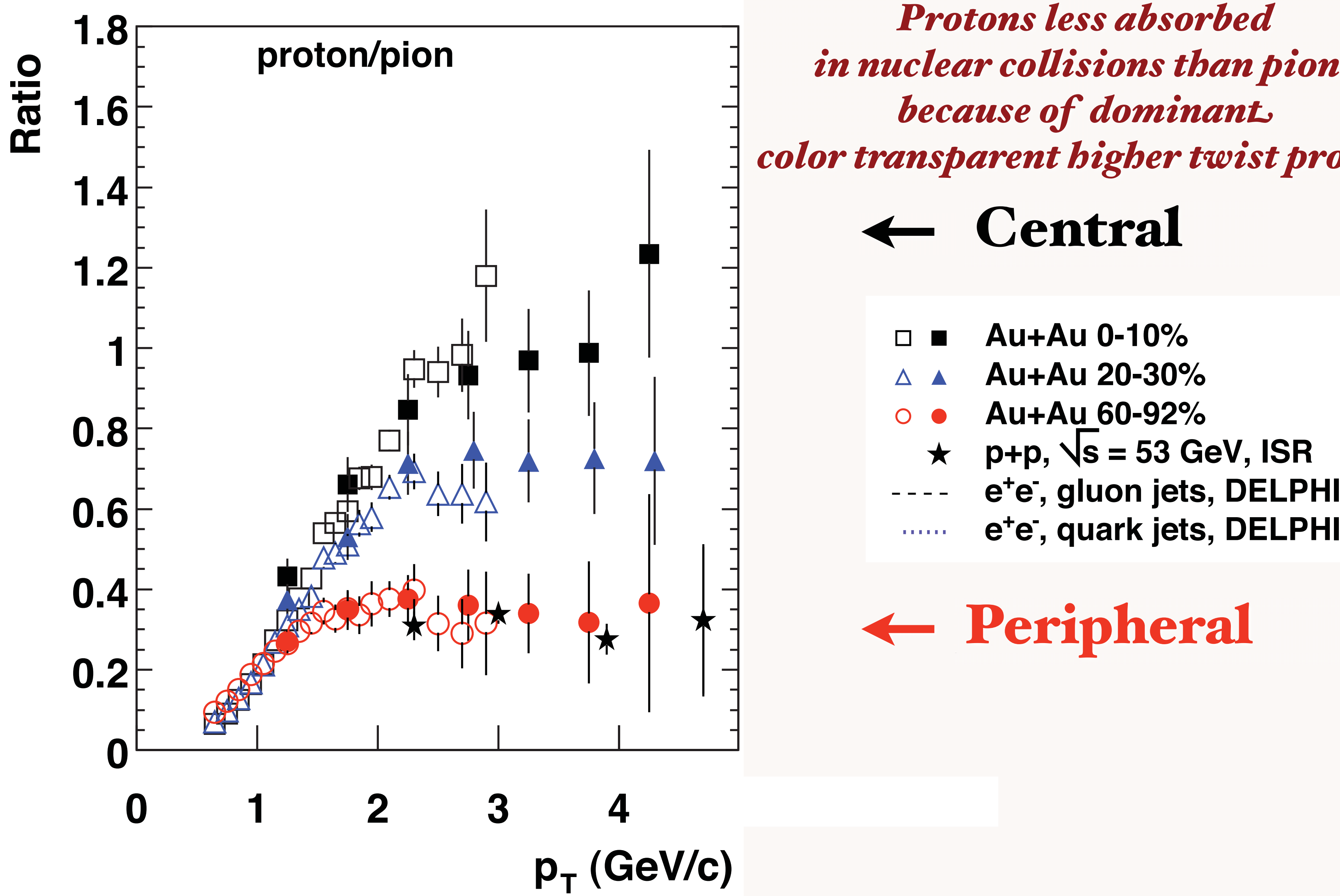

Protons less absorbed in nuclear collisions than pions because of dominant color transparent higher twist process

← **Central**

← **Peripheral**

Anne Sickles

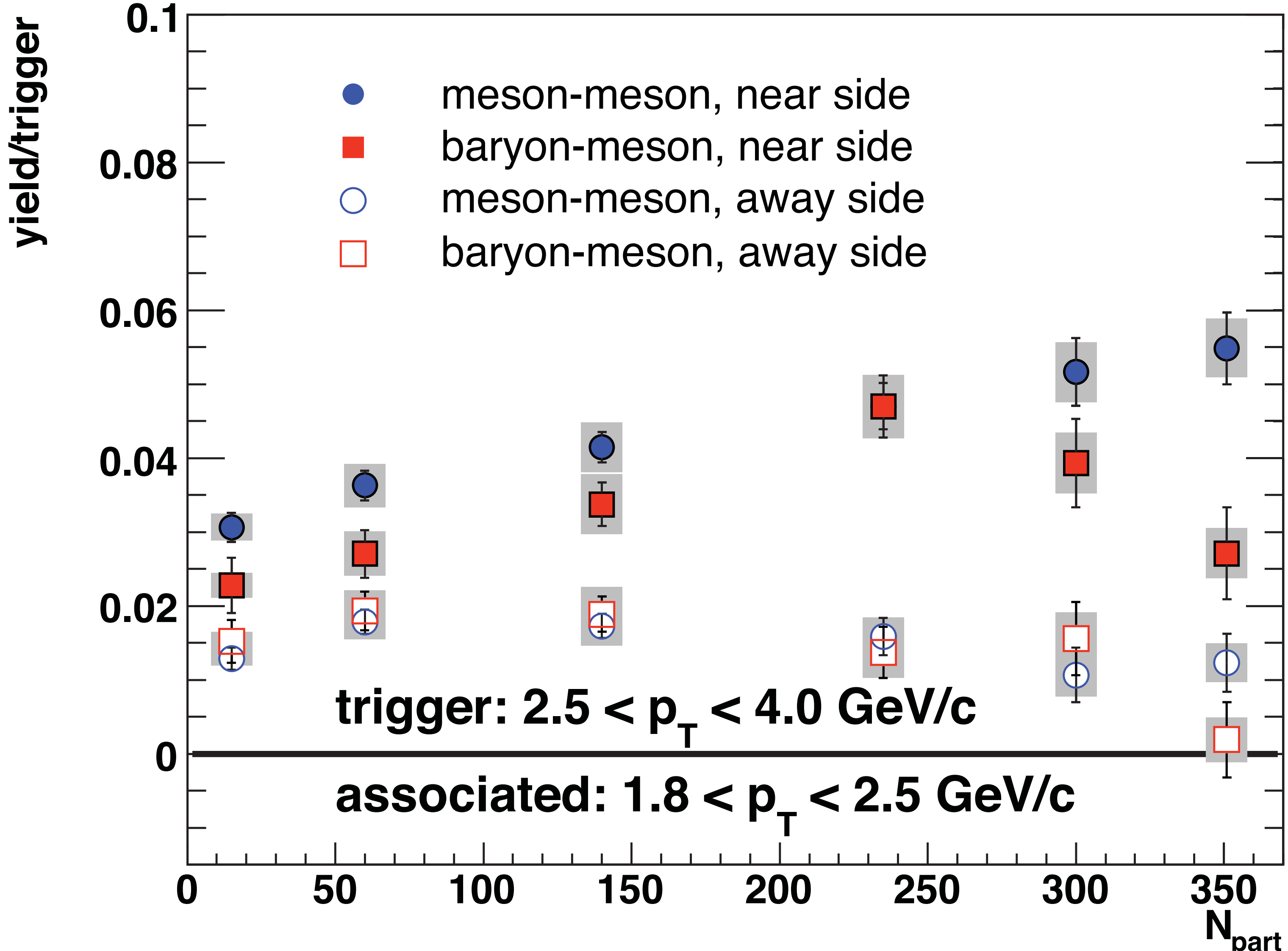

proton trigger: # same-side particles decreases with centrality

Proton production more dominated by color-transparent direct high-n_{eff} subprocesses

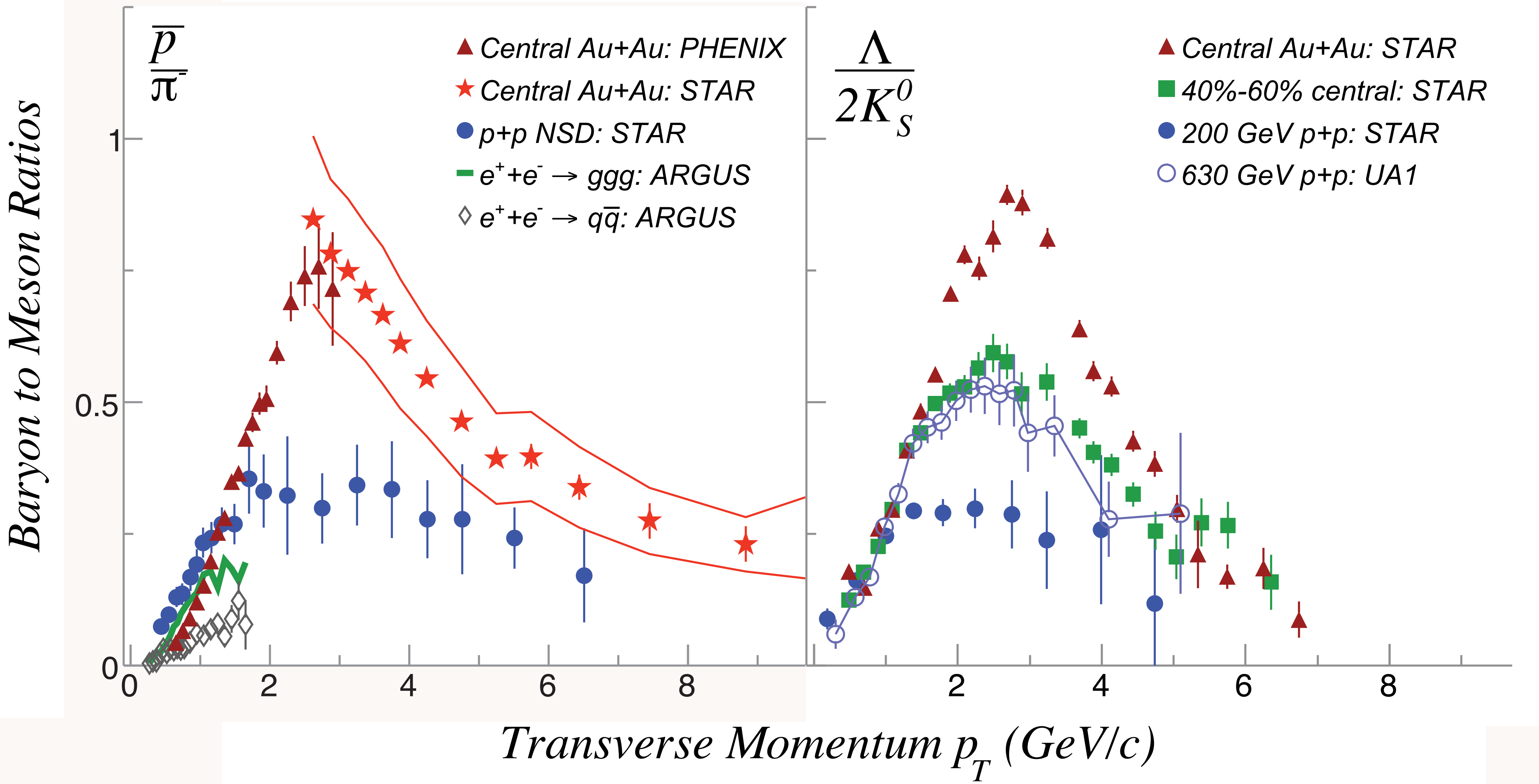
$\frac{\bar{p}}{\pi^-}$
Central Au+Au: PHENIX
Central Au+Au: STAR
p+p NSD: STAR
$e^+ + e^- \rightarrow ggg$: ARGUS
$e^+ + e^- \rightarrow q\bar{q}$: ARGUS
$\frac{\Lambda}{2K^0_S}$
Central Au+Au: STAR
40%-60% central: STAR
200 GeV p+p: STAR
630 GeV p+p: UA1
Baryon to Meson Ratios
Transverse Momentum p_T (GeV/c)
0
0.5
1
0
2
4
6
8

Power-law exponent $n(x_T)$ for π^0 and h spectra in central and peripheral Au+Au collisions at $\sqrt{s_{NN}} = 130$ and 200 GeV

S. S. Adler, *et al.*, PHENIX Collaboration, *Phys. Rev.* C **69**, 034910 (2004) [nucl-ex/0308006].

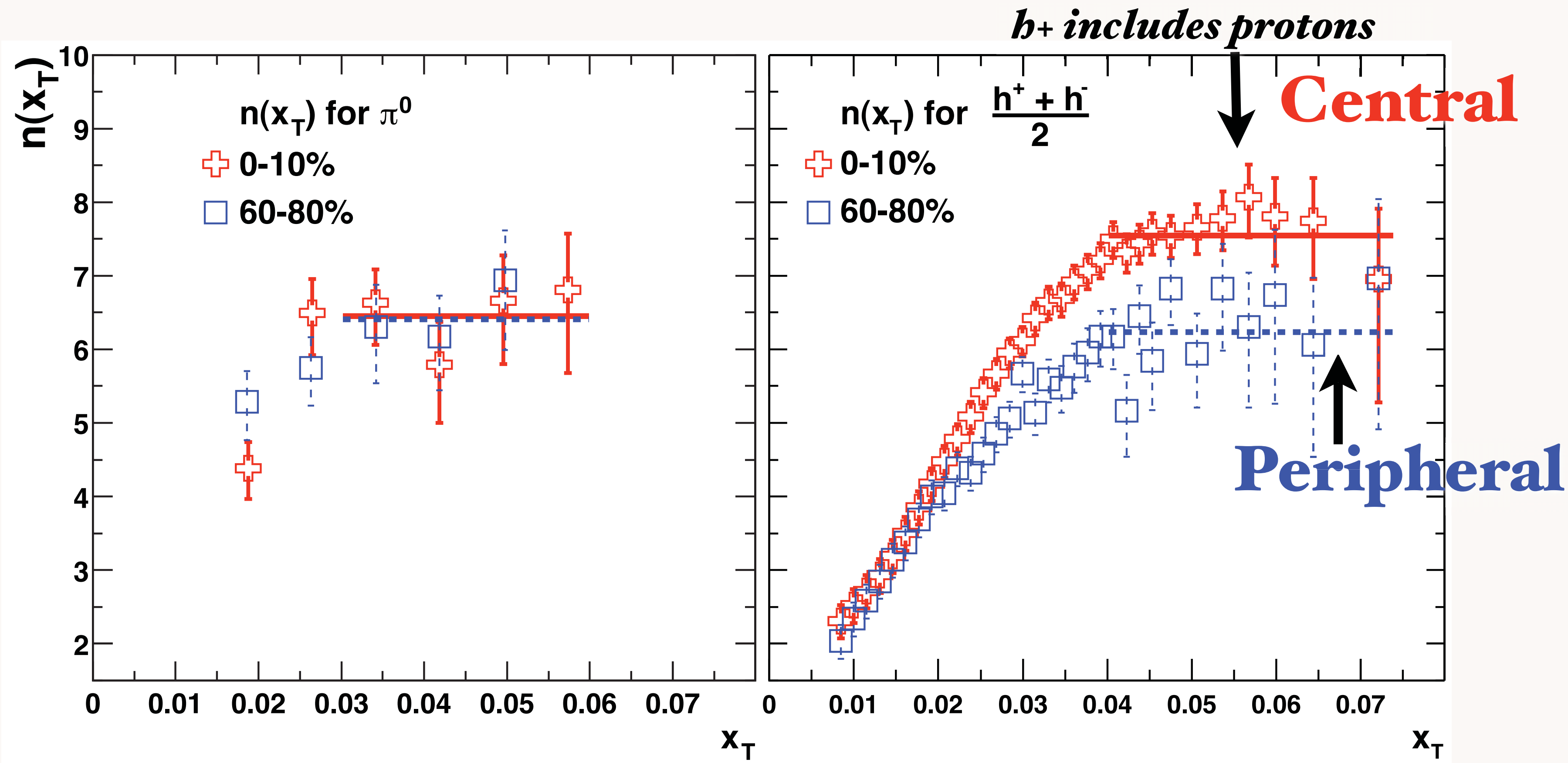

Proton production dominated by color-transparent direct high n_{eff} subprocesses

Lambda can be made directly within hard subprocess

Coalescence within hard subprocess

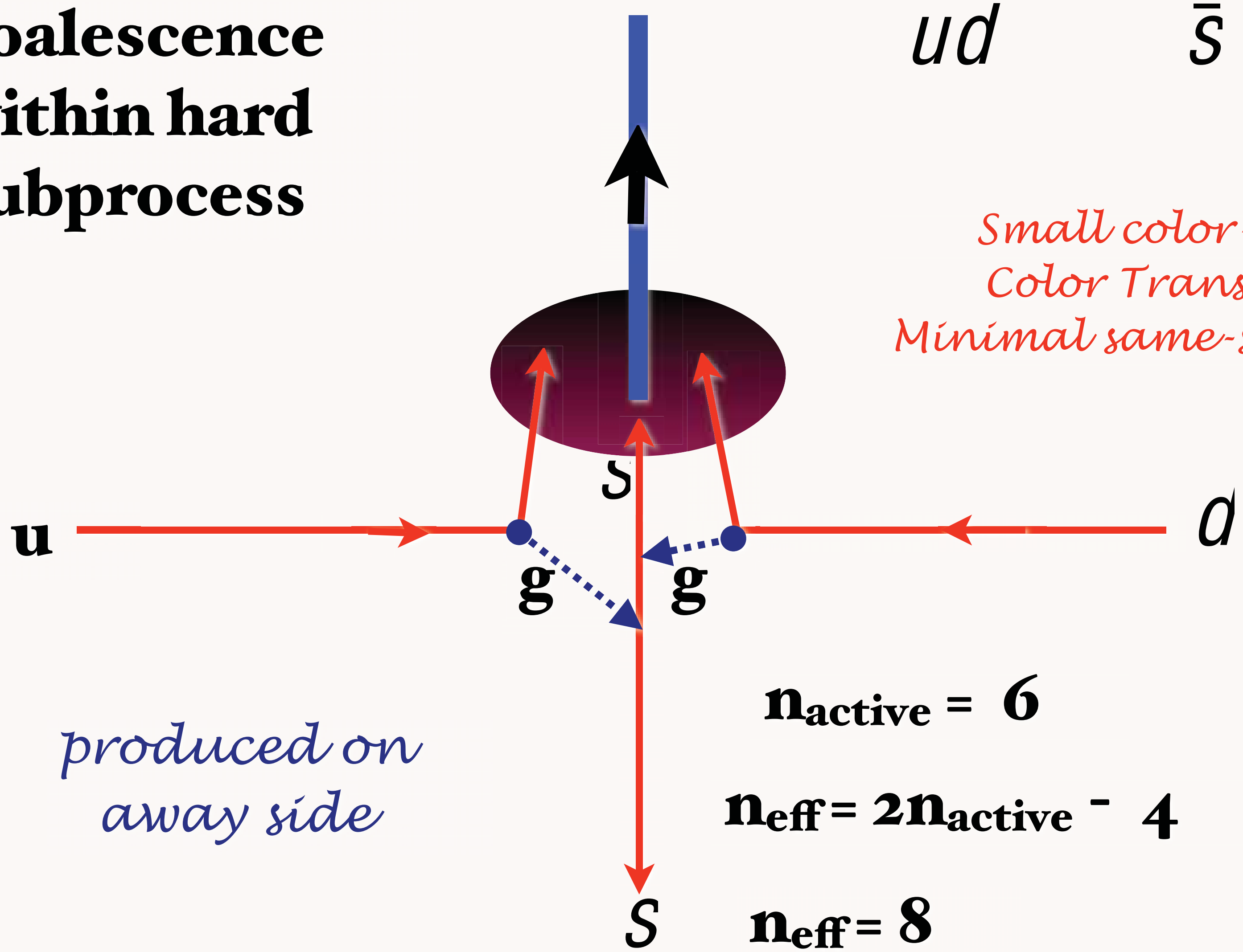

Small color-singlet
Color Transparent
Minimal same-side energy

s *produced on away side*

$\mathbf{n_{active} = 6}$

$\mathbf{n_{eff} = 2n_{active} - 4}$

$\mathbf{n_{eff} = 8}$

Sickles, sjb

Baryon Anomaly: Evidence for Direct, Higher-Twist Subprocesses

- Explains anomalous power behavior at fixed x_T
- Protons more likely to come from direct higher-twist subprocess than pions
- Protons less absorbed than pions in central nuclear collisions because of color transparency
- Predicts increasing proton to pion ratio in central collisions
- Proton power n_{eff} increases with centrality since leading twist contribution absorbed
- Fewer same-side hadrons for proton trigger at high centrality
- Exclusive-inclusive connection at $x_T = 1$

New Perspectives for QCD from AdS/CFT

- LFWFs: Fundamental frame-independent description of hadrons at amplitude level
- Holographic Model from AdS/CFT : Confinement at large distances and conformal behavior at short distances
- Model for LFWFs, meson and baryon spectra: many applications!
- New basis for diagonalizing Light-Front Hamiltonian
- Physics similar to MIT bag model, but covariant. No problem with support $0 < x < 1$.
- Quark Interchange dominant force at short distances

CIM: Blankenbecler, Gunion, sjb

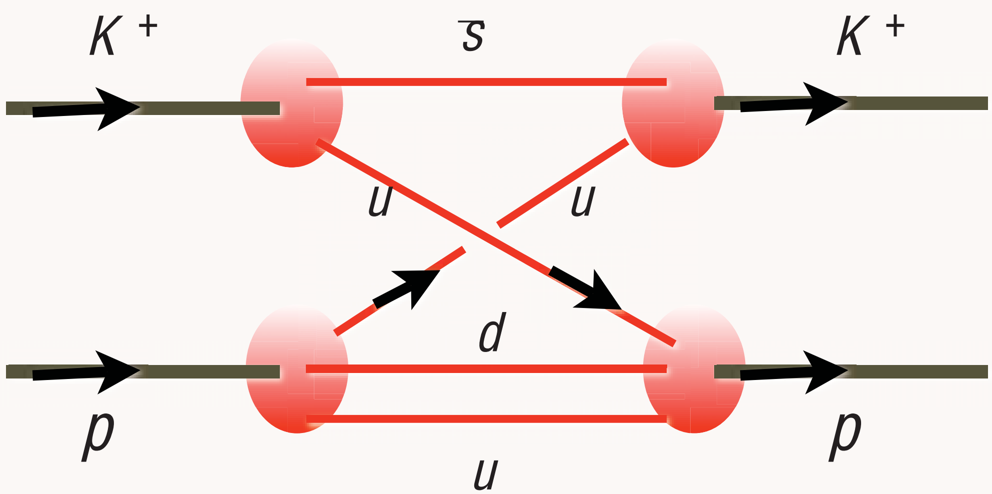

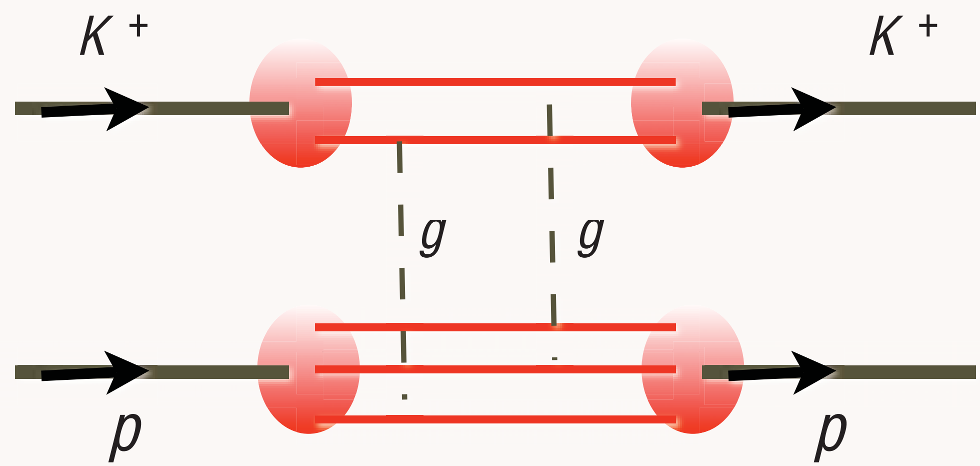

Quark Interchange
(Spin exchange in atom-atom scattering)

Gluon Exchange
(Van der Waal -- Landshoff)

$$\frac{d}{dt} = \frac{|M(s,t)|^2}{s^2}$$

$M(t,u)_{\text{interchange}} \quad \frac{1}{ut^2}$

$M(s,t)_{\text{gluonexchange}} \quad sF(t)$

MIT Bag Model (de Tar), large N_C, ('t Hooft), AdS/CFT all predict dominance of quark interchange:

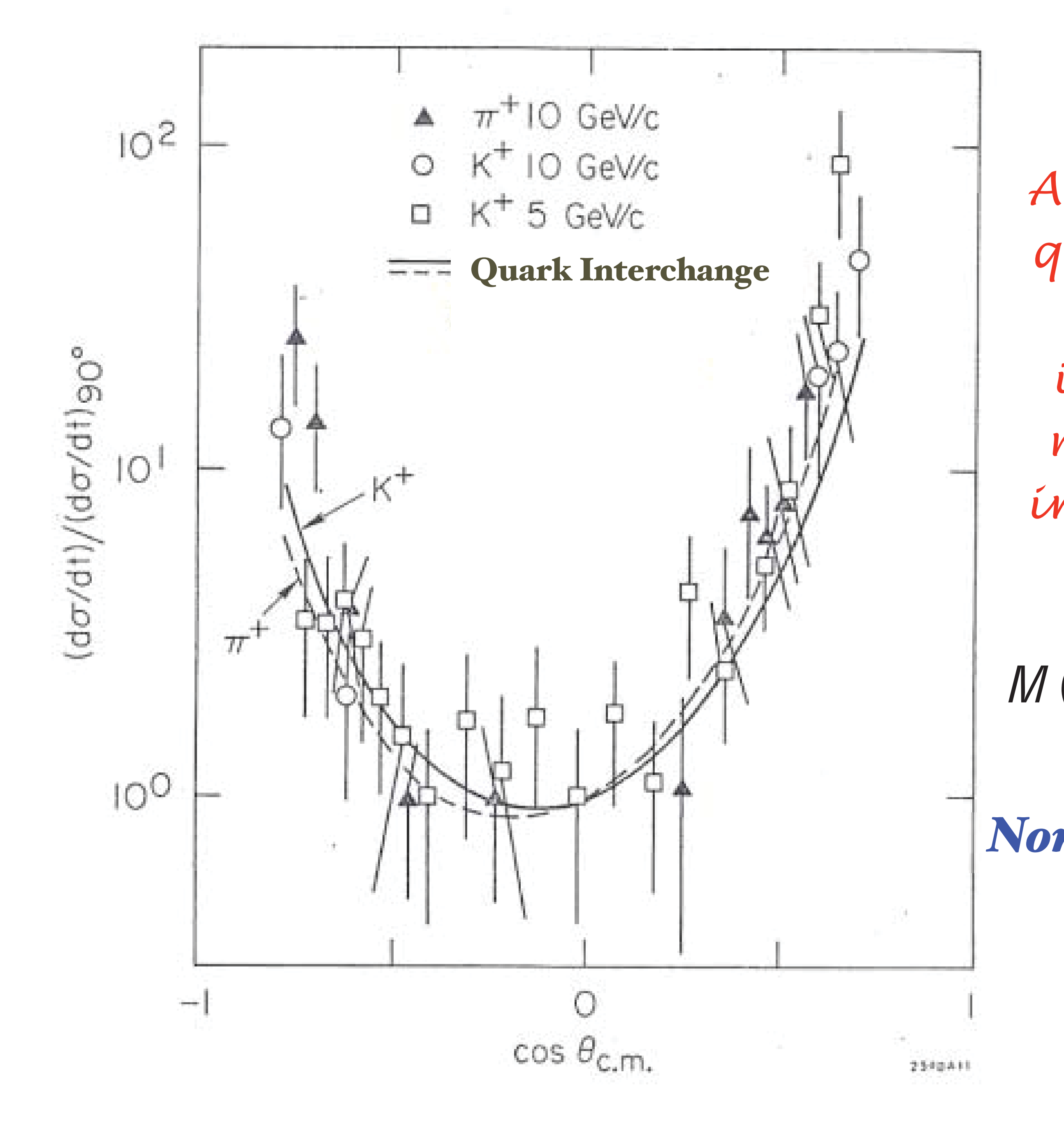

AdS/CFT explains why quark interchange is dominant interaction at high momentum transfer in exclusive reactions

$$M(t,u)_{\text{interchange}} \quad \frac{1}{ut^2}$$

Non-linear Regge behavior:

$$_R(t) \quad -1$$

Comparison of Exclusive Reactions at Large t

B. R. Baller,[a] G. C. Blazey,[b] H. Courant, K. J. Heller, S. Heppelmann,[c] M. L. Marshak, E. A. Peterson, M. A. Shupe, and D. S. Wahl[d]
University of Minnesota, Minneapolis, Minnesota 55455

D. S. Barton, G. Bunce, A. S. Carroll, and Y. I. Makdisi
Brookhaven National Laboratory, Upton, New York 11973

and

S. Gushue[e] and J. J. Russell
Southeastern Massachusetts University, North Dartmouth, Massachusetts 02747
(Received 28 October 1987; revised manuscript received 3 February 1988)

Cross sections or upper limits are reported for twelve meson-baryon and two baryon-baryon reactions for an incident momentum of 9.9 GeV/c, near 90° c.m.: $\pi^{\pm}p \rightarrow p\pi^{\pm}, p\rho^{\pm}, \pi^{+}\Delta^{\pm}, K^{+}\Sigma^{\pm}, (\Lambda^{0}/\Sigma^{0})K^{0}$; $K^{\pm}p \rightarrow pK^{\pm}$; $p^{\pm}p \rightarrow pp^{\pm}$. By studying the flavor dependence of the different reactions, we have been able to isolate the quark-interchange mechanism as dominant over gluon exchange and quark-antiquark annihilation.

$\pi^{\pm}p \rightarrow p\pi^{\pm}$,

$K^{\pm}p \rightarrow pK^{\pm}$,

$\pi^{\pm}p \rightarrow p\rho^{\pm}$,

$\pi^{\pm}p \rightarrow \pi^{+}\Delta^{\pm}$,

$\pi^{\pm}p \rightarrow K^{+}\Sigma^{\pm}$,

$\pi^{-}p \rightarrow \Lambda^{0}K^{0}, \Sigma^{0}K^{0}$,

$p^{\pm}p \rightarrow pp^{\pm}$.

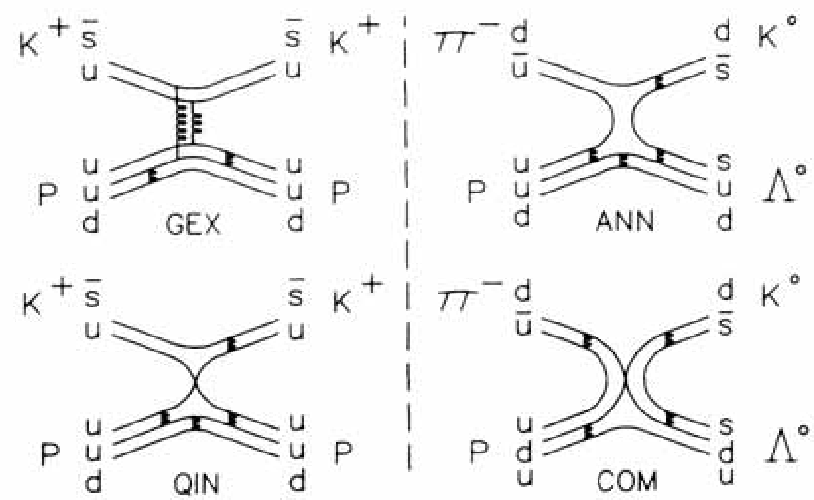

Hadron Dynamics at the Amplitude Level

- LFWFS are the universal hadronic amplitudes which underlie structure functions, GPDs, exclusive processes, distribution amplitudes, direct subprocesses, hadronization.
- Relation of spin, momentum, and other distributions to physics of the hadron itself.
- Connections between observables, orbital angular momentum
- Role of FSI and ISIs--Sivers effect
- Higher Fock States give GMOR Relations, Chiral Symmetry Breaking

Features of Soft-Wall AdS/QCD

- Single-variable frame-independent radial Schrodinger equation
- Massless pion (m_q =0)
- Regge Trajectories: universal slope in n and L
- Valid for all integer J & S. Spectrum is independent of S
- Dimensional Counting Rules for Hard Exclusive Processes
- Phenomenology: Space-like and Time-like Form Factors
- LF Holography: LFWFs; broad distribution amplitude
- No large Nc limit
- Add quark masses to LF kinetic energy
- Systematically improvable -- diagonalize H_{LF} on AdS basis

String Theory

↓

AdS/CFT

Mapping of Poincare' and Conformal SO(4,2) symmetries of 3+1 space to AdS5 space

↓

AdS/QCD

Goal: First Approximant to QCD

Counting rules for Hard Exclusive Scattering

Regge Trajectories

QCD at the Amplitude Level

Conformal behavior at short distances

+ Confinement at large distance

↓

Semi-Classical QCD / Wave Equations

↓

Holography

Boost Invariant 3+1 Light-Front Wave Equations

↓

J =0,1,1/2,3/2 plus L

Integrable!

Hadron Spectra, Wavefunctions, Dynamics